STEAM GASIFICATION OF SIBERIAN ELM

by

GANESAN SUNDAR

B.Tech. Indian Institute of Technology, Madras, 1985

A MASTER'S THESIS

submitted in partial fulfillment of the
requirements for the degree

MASTER OF SCIENCE

Department of Chemical Engineering

KANSAS STATE UNIVERSITY
Manhattan, Kansas

1988

Approved by

Walter P Walawender

Major Professor

ACKNOWLEDGEMENTS

I take this opportunity to express my sincere gratitude to my major professor, Dr. W. P. Walawender for his able guidance, valuable help and encouragement in all stages of my work.

I wish to express my thanks to Dr. L. T. Fan and Dr. L. A. Glasgow for serving as members of my supervisory committee.

I am also indebted to my colleagues of the Pyrolysis Seminar Group for their valuable suggestions and help during the course of my work.

Finally, I wish to acknowledge the Engineering Experiment Station (Hydrogen Project), and the Department of Chemical Engineering,of Kansas State University for the financial support.

TABLE OF CONTENTS

CHAPTER 1

INTRODUCTION

The projected diminishing supply of crude oil coupled with our growing dependence on foreign oil prompted a search for alternate energy sources. Woody biomass constitutes a major source of alternate energy. Thermal conversion is one of the more popular technical options for the conversion of this carbonaceous solid into more convenient forms of energy. Gasification is the particular type of thermochemical conversion that is of interest in this thesis. Among the various contacting devices used for gasification, the fluidized bed has been selected for study because of its advantageous features of excellent gas-solid contacting and high heat transfer rate.

Steam gasification provides a means for converting wood into a hydrogen-rich gas that can be employed as fuel gas or as synthesis gas. The synthesis gas composition can be adjusted by adjusting some gasification parameters, such as the steam-to-feed ratio.

The principal objectives of this thesis are (1) to experimentally determine the effect of steam-to-feed ratio on the gasification of Siberian elm in a fluidized bed and (2) to develop a mathematical model to describe the gasification process in the experimental reactor.

Chapter II presents background information along with a review of the gasification literature of various species of wood. The review includes the kinetics of gasification,

descriptions of various studies on the influences of various operating parameters and a survey of previous modeling efforts.

Chapter III presents the results of the experimental study on the influence of the steam-to-feed ratio on the gasification of Siberian elm. The results have been explained on the basis of water-gas shift reaction; subsequently, the effects of steam-to-feed ratio on gasification characteristics are discussed. The characteristics of interest were the gas composition, the higher heating value of the product gas, the volumetric and mass yields of gas, the energy recovery and the carbon conversion.

Chapter IV presents a two-phase model to describe the experimental fluidized-bed gasification process. The model included devolatilization, the char gasification reactions, the water-gas shift reaction, and the freeboard reactions. Both dynamic and steady gas compositions are simulated and compared with the experimental observations.

Chapter V summarizes the major conclusions of the thesis and presents recommendations for extension of the work.

CHAPTER 2

BACKGROUND AND LITERATURE REVIEW

The projected depletion of crude oil has given rise to a search for alternate energy sources. Utilization of agricultural and forest biomass has been of interest in this regard, mainly because of the abundance of these renewable energy resources. Woody biomass constitutes the major source of terrestrial biomass.

Wood has been used as fuel from time immemorial. During the later part of the nineteenth century, wood was the major source of energy in the U.S., supplying three fourths of the energy demand. Since that time, there has been large scale increases in the energy demand, a large increase in the utilization of fossil fuels, and diminishing use of wood for energy (Seamann, 1977).

The potential of wood as an alternate source of energy can be appreciated by examining its availability. Presently, about 6% of the earth's land area is cultivated, out of which about 1% is utilized for food production. (Cheremisinoff, 1980). This implies that the vast renewable remainder can be conveniently converted to utilizable forms of energy and chemicals.

An overall material balance analysis on the forest products industries also reveals the vast energy potential of wood. For example, in 1970, the plywood industry consumed about 105 million metric tons of roundwood to produce about 37 million metric tons of finished product.

This indicates processing wastes amounting to 68 million metric tons. Out of this, about 44 million metric tons were used as fuel and feedstock and about 24 million metric tons were wastes (Soffer, 1981). Assuming an average heating value of 19 MJ/kg, it can be estimated the plywood industry wastes have an energy equivalent of 0.5 EJ (10^{18} J). In fact, the lowest estimates of annual energy production from wood residues can be as high as 2 to 5 EJ (Smil, 1983).

Recognizing the vast energy potential of wood, approaches have been recently developed to increase wood production in a controlled manner. The method that has received much attention in the past decade is the short rotation energy plantation concept. As a consequence of the high wood yield and young harvest age, this source of woody biomass can provide a major source of fuel (Geyer, 1981). Several species including the poplars (Populus), maples (Acer), locust (Robinia), and alders (Alnus) have been identified for this program.

THERMOCHEMICAL CONVERSION OF WOOD

The various conversion technologies that have been suggested for producing wood-derived energy products is presented in Figure 2.1. (Cheremisinoff, 1980). One of the major options for transforming wood to more convenient forms of energy is through thermochemical conversion. This technology involves use of elevated temperatures.

Combustion, pyrolysis and gasification all fall under this classification.

Gasification may be defined as the process by which organic materials are converted, in a reactive atmosphere, into a gaseous phase comprised of H_2, H_2O, CO, CO_2, CH_4, and trace amounts of light hydrocarbons. Solid residue and tar are also obtained. The amounts of char and tar decrease with an increase in the gasification temperature as a consequence of secondary reactions. Pyrolysis differs from gasification in that it refers to thermal decomposition in an inert atmosphere. Pyrolysis is the first step in both gasification and combustion. Combustion is a limiting case in which the pyrolysis products are oxidized in an oxygen rich atmosphere.

Gasification is highly desirable in that it yields a gaseous product that can be easily handled; also pollution hazards are reduced in gasification compared to combustion. Total gasification of the solid is most desirable in almost all gasification processes. The low ash content and high volatility of wood makes gasification of wood highly desirable.

There are a variety of reactors that can be used for gasification, the more important of them being the fixed/moving beds, entrained beds and fluidized beds. Fluidized beds provide isothermal conditions that allow good process control. Moreover, they can function with a wide variation

in the feed material properties. Vigorous mixing in the emulsion phase results in high heat and mass transfer rates.

CHEMICAL COMPOSITION OF WOOD

Knowledge of the chemical constituents of wood is important for interpreting the results of thermochemical experiments. Wood is composed of a variety of substances, the chief constituents being cellulose, lignin and hemicellulose. Cellulose, a high molecular weight water insoluble straight chain polymer, accounts for nearly 50% by weight of the wood substance. Cellulose is readily degradable by thermal treatment. Lignin, the next major constituent is basically an insoluble material, loosely bonded to the cellulose. The lignin content varies between wood species; in general, softwood has more lignin than hardwood. Lignin requires vigorous treatment for devolatilization. Hemicelluloses are formed of simple sugar molecules; they are thermally much more reactive than lignin.

There are over a 100 different tree species in the U.S. All of them have a low ash content, usually less than 2% for the wood. Wood is also low in sulphur content. (Mullen, 1970, Junge, 1975). This eliminates sulphur dioxide problems. Volatiles account for 80 to 90 percent by weight (dry basis) in almost all wood types (Mingle and Boubel,

1968). The variation in vloatility is due in part to differences in the contents of the three constituents.

Wood, with an average heating value of 19 MJ/kg, has about one-third lower energy content compared to standard coal (29.3 MJ/kg). However, wood is much more volatile than coal.

REACTION MECHANISMS IN GASIFICATION

Biomass gasification has been studied in detail by Antal et al. (1978). He has proposed that gasification occurs in three stages (1) Pyrolysis or devolatilization which produces volatile matter (tar and gas) and char (2) secondary reactions involving the evolved volatiles and (3) gasification of char. Based on that, Raman et al. (1981) developed a conceptual scheme to describe the reaction path for gasification of carbonaceous material based on Antal's work. The scheme can be visualized as shown in Figure 2.2.

In the case of rapid heating of small particles, the devolatilization step is nearly instantaneous. The heavy volatiles can subsequently crack to form lighter volatiles and gas. The char can also react with H_2, CO and H_2O to produce additional gas.

GASIFICATION STUDIES

At present the gasification of wood is not practiced extensively on a commercial scale. However, it has been

studied by various researchers under various conditions. Variations in the gasifier operating parameters and in the reactive environment can result in different product distributions. This necessitates a systematic study of the influence of the operating parameters on gasification processes.

Fluidized-bed gasification of wood has been investigated for more than 30 years (Morgan et al. (1953), Huffman and Lin (1977), Epstein et al.(1978)). In general, previous studies have identified that temperature, volatiles residence time, heating rate, and particle size are important parameters affecting the gasification characteristics of wood and other biomass. Burton (1972), Feldman et al. (1981), Walawender and Fan (1978) and Raman et al. (1980) have conclusively shown that temperature is a major factor influencing gasification. The effect of residence time of the volatiles on product gas composition has been discussed in detail by Antal (1979), Rensfelt (1978) and Rose (1982). The effects of high heating rates on pyrolysis and hydropyrolysis have been studied by Eklund (1982).

Other parameters have not been studied systematically; one of them being the steam-to-feed ratio. However, there have been some efforts in the past to investigate the effect of steam on the fluidized-bed gasification of biomass. These works will be reviewed in the following section.

Effect of Steam on Gasification

Beck et al. (1979) studied gasification of feedlot manure in a pilot-scale fluidized-bed reactor. The fluidizing medium was a mixture of air and steam and the operating temperature was maintained at 975 K. The product gas contained significant amounts of CO, CO_2, H_2, and CH_4. They also gasified oak sawdust in the same reactor and found that the gas yield for wood was higher than for manure (Beck et al., 1980). Multiple regression analysis of both data sets, assuming that the gas yield depended upon both temperature and the air-to-DAF feed ratio, gave better correlation than by correlating gas yield to temperature alone. They also found that for their temperature range (below 1075 K), the steam-char reaction was not significant.

Antal et al. (1978) investigated the secondary reactions of wood and cellulose generated volatiles in a quartz plug flow reactor. They studied the effect of steam-to-feed ratio (up to 1.4) on the gasification and concluded that there was no significant effect; they stated that gasification is dominated by tar cracking reactions and that steam reforming reactions are not important for temperatures below 1023 K. On the other hand, Rensfelt et al. (1978) studied the flash pyrolysis of poplar wood and concluded that steam reacts with the gaseous hydrocarbon products and solid char.

Schoeters et al. (1981) gasified linden wood shavings with air and steam in a bench-scale (0.15 cm ID) fluidized-bed reactor. The temperature range was limited to 900 and 1100 K. They found that the higher heating value of the off-gas ranged from 4 to 5 MJ/m^3 and that the optimum energy recovery was about 60%. They also found that high steam rates lowered the gas HHV, the gas yield and the energy recovery. An investigation of the influence of freeboard temperature on the gas yield, revealed an increase in CO_2 and H_2 concentrations and a CO concentration decrease with increase in temperature. They explained all their results on the basis of the water-gas shift reaction and indicated that the CO concentration should increase above 1123 K due to the reversal of the direction of the shift reaction.

Feldman et al. (1981) used a multi-solid fluidized-bed gasifier (6 in. ID) to gasify wood chips. The temperature of the bed was varied between 920 K and 1200 K. An increase in the temperature resulted in an increase in the carbon conversion (to about 85% at the highest temperature) and a maximum in the product heating value. Also, an increase in the wood chip moisture content resulted in a decrease in the carbon conversion. From their studies on the effect of steam-to-feed (S/F) ratio (up to 0.8 lb steam per lb dry wood), it was concluded that the carbon conversion was not affected and that there was no net steam consumption. Even

with the excess steam used, the H_2/CO ratio obtained was much lower than the equilibrium ratio.

Walawender et al. (1982) investigated the steam gasification of alpha cellulose in a 2 inch fluidized-bed reactor with a mixture of limestone and sand bed material. Steam was the sole fluidizing agent. Based on their data, a conceptual model was developed which indicated that the overall process can be considered to be composed of two steps; devolatilization and secondary gas phase reactions. While the former is almost instantaneous for small particles in a fluidized bed, the latter takes place in two regimes: a tar cracking dominated regime up to 940 K and a water-gas shift reaction dominated regime above 940 K. The results from their experiments showed a sharp transition between the two regimes. They inferred that steam, when present in large excess, actively particlipates in the gasification process through the shift reaction.

Singh (1986) studied the gasification of cottonwood in the same reactor as that of Walawender et al. His results were in accord with the conceptual model proposed by Walawender et al. (1982). However, the transition from one regime to the other was not as sharp as the case of alpha cellulose.

Walawender et al. (1985a) also studied the effect of elevated freeboard temperatures on the steam gasification of cellulose in a steam fluidized-bed reactor. The operating

temperature range was 865 to 1060 K. The freeboard temperature was maintained at 50-100 K higher than the bed temperature. The gas yield, energy recovery, and carbon conversion trends were not affected by the temperature elevation. Furthermore, the slopes of the gas composition-temperature plots did not change for the higher freeboard temperatures. Based on their observations, the authors claimed additional support for the hypothesis of the water-gas shift dominated regime.

Walawender et al. (1985b) also studied the influence of steam-to-feed ratio on the gasification of Siberian elm at temperatures from 850 K to 1160 K at atmospheric pressure. In this preliminary work, they statistically compared regression models for the gasification characteristics with temperature as the independent variable and steam-to-feed ratio as a parameter. Whenever it was possible to make comparisons, it was found that a significant difference existed between the gasification charcteristics for different steam-to-feed ratios.

Effect of Catalysts

Some research efforts have been directed at the use of catalysts to promote the formation of gaseous products with specific H_2/CO ratios. Additionally, some of these efforts have considered the effect of steam on the gasification characteristics; hence, a review of this topic is in order.

Degroot and Shafizadeh (1982) studied various factors controlling the gasification of biomass chars, including the effects of steam and catalysts. Their samples included chars from Douglas fir heartwood and cottonwood sapwood. The gasification temperature was about 1300 K. They found that the overall kinetics could be approximated by a zero order Arrhenius rate expression in which the rate was dependent on the initial mass of the sample. They also found that alkali metals lowered the apparent activation energy for both the char-CO_2 and char-steam gasification reactions.

Hallen et al. (1982) also investigated the influence of alkali carbonates on biomass gasification. From their results, they inferred that at temperatures of about 825 K, the devolatilization step is complete but carbon gasification is slow without the presence of catalysts. Addition of the alkali catalyst increases the gas yield due to char gasification. They also concluded that these catalysts enhanced the water-gas shift reaction significantly.

Baker et al. (1982) have discussed the influence of catalysts on the gas phase reactions in the steam gasification of biomass. They were interested in determining the best catalyst for the production of methane-rich, hydrogen-rich and methanol synthesis gases. For producing the hydrogen rich gas, they determined that metal

oxides (Fe, Cr, Cu, Zn) favored the water-gas shift reaction.

Development of Mathematical Models

There have been a few studies directed at the development of models for gasification of wood. The models vary considerably in their sophistication; they range from simple equilibrium models to complex three phase fluidized-bed models. Most investigations have made some attempt to compare their predictions with limited experimental data.

Particle models. Research in this area has been conducted at the University of Aston at Birmingham (Hatt, 1982). They developed a particle gasification model based on the work of Groenveld (1980). The particles are assumed to be spherical, porous and isothermal. The gasifying agents investigated were CO_2 and steam. The only reactions considered were those between the gasifying agents and the particle and the water-gas shift reaction, with the shift reaction acting homogeneously throughout the particle.

Maa and Bailey (1978) modeled the isothermal pyrolysis of wood particles in a fluidized-bed reactor based on the shrinking core model. The time for complete reaction of the solid was determined but no effort was made to predict the product gas composition.

Two phase models. Since the present work is aimed at developing a two phase model for the gasification of wood in

a fluidized-bed reactor, attention will be focused on the related foundations for the present work. Most of the two phase models have been based on either the Kunii-Levenspiel model (1969) or the Davidson-Harrison model (1971).

Yoshida and Kunii (1974) modeled the gasification of carbon with air and steam. They based their model on the K-L two phase theory. Assuming pseudo-first order kinetics for the char gasification reactions and the water-gas shift reaction to be in equilibrium, they simulated gas compositions. The char gasification reactions included the reaction of char with O_2, CO_2, and steam. The model only considered the bed section and did not account for the reactions in the freeboard. They compared their simulated results with experimentally determined compositions; reasonable agreement was obtained by variation of system parameters. Their model had the following major limitations: 1) The predictions depended heavily on some hydrodynamic parameters for which correlations had not yet been developed. Only by adjusting the parameters were suitable fits of the model to the experimental observations obtained. 2) Experimental observations have indicated that the water-gas shift equilibrium is usually not approached in fluidized-bed gasifiers until the gasifier reaches very high temperatures.

Bacon and Downie (1982) developed a model for the fluidized-bed gasification of wood, based on the bubble

assemblage model. Their model included devolatilization, char gasification reactions and the water-gas shift reaction. They assigned degrees of equilibrium for the char gasification reactions. They stated that a comparison of the simulated runs with some industrial data showed fairly good agreement. The major limitation of their model is that the kinetics are not included.

Raman et al. (1981) developed a model to simulate the behavior of a fluidized bed for biomass gasification and applied it to simulate experimentation with feedlot manure. The model included the char gasification and water-gas shift reactions in addition to devolatilization. No elutriation of char was considered. A comparison of the steady gas compositions with their experimental results showed good agreement. Chang et al. (1983) extended this work to provide information on the dynamic behavior of the fluidized-bed gasifier. The major limitation of this model is that freeboard reactions are not included.

CONCLUDING REMARKS

From the reviews presented, it is evident that several factors affect the gasification of biomass; however, the effect of some of them is not clear. Temperature affects the process the most. Other factors such as gas residence time, particle size, heating rate, appear to influence the product yield. In the case of steam gasification, with evidence for

the water-gas shift reaction domination, the steam-to-feed ratio can be a significant factor affecting the process. The present work was conducted in an effort to clarify the effect of steam-to-feed ratio on steam gasification of Siberian elm. It was also directed at developing a mathematical model for the fluidized-bed gasification of wood which includes devolatilization, char gasification reactions, water-gas shift reactions and freeboard reactions.

REFERENCES

Antal, M. J., W. E. Edwards, W. E. Friedman and F. E.Rogers, "A Study of the Steam Gasification of Organic Wastes," Project Report to EPA, W. W. Liberick, Project Officer, Industrial Environment Research Laboratory, Cincinatti, Ohio, 1978.

Antal, M. J., "The Effects of Residence Time, Temperature, and Pressure on the Steam Gasification of Biomass," presented at the Symposium on Biomass as a Non-Fossil Fuel Source, Div. of Fuel Chem. ACS Meeting, Honolulu, Apr. 1-6, 1979.

Bacon, D. W., J. Downie, J. C. Hsu, and J. Peters, "Modeling of Fluidized Bed Wood Gasifiers," presented at the Fundamentals of Thermochemical Biomass Conversion Conference, Estes Park, CO, Oct 18-22, 1982.

Baker, E. G., L. K. Mudge, and W. A. Wilcox, "Catalysis of Gas Phase Reactions in Steam Gasification of Biomass," presented at the conference on the Fundamentals of Thermochemical Biomass Conversion, Estes Park, CO, Oct 18-22, 1982.

Beck, S. R., W. J. Huffman, B. L. Landeene, and J. Halligan, "Pilot Plant Results for Partial Oxidation of Cattle Feedlot Manure," Ind. Eng. Chem. Process Des. Dev., 18 (2), 328-332 (1979).

Beck, S. R., and M. J. Wang, "Wood Gasification in a Fluidized Bed," Ind. Eng. Chem. Process Des. Dev., 19, 312-317 (1980).

Burton, R. S., "Fluid Bed Gasification of Solid Waste Materials," M. S. Thesis, West Virginia University, 1972.

Chang, C. C., L. T. Fan, and W. P. Walawender, "Dynamic Modeling of Biomass Gasification in a Fluidized Bed," presented at 1983 AIChE Annual Meeting, Washington, D. C., Oct30-Nov4, 1983.

Cherimisinoff, N. O., "Wood for energy Production," Energy Technology Series, Ann Arbor Science, p 22, 1980.

Davidson, J., and D. Harrison, "Fluidization," Academic Press, New York, 1971.

Degroot, W. F., and F. Shafizadeh, "Kinetics of Wood Gasification by Carbon Dioxide and Steam," presented at

the Fundamentals of Thermochemical Biomass Conversion Conference, Estes Park, CO, Oct 18-22, 1982.

Eklund, H., and W. Wanzl, "Pyrolysis and Hydropyrolysis of Peat at High Heating Rates," presented at the Fundamentals of Thermochemical Biomass Conversion Conference, Estes Park, CO, Oct 18-22, 1982.

Epstein, E., H. Kosstrin, and Joel Alpert, "Potential Energy Production in Rural Communities From Biomass And Wastes Using A Fluidized Bed Pyrolysis System," presented at the symposium on Energy From Biomass And Wastes, Aug 14-18, Washington, D.C., 1978.

Feldmann, H. F., P. S. Choi, M. A. Paisley, S. P. Chauhan, C. J. Robb, D. W. Folsom, and B. C. Kim, "Steam Gasification of Wood in a Multi Solid Fluidized Bed Gasifier," presented at the symposium on Energy From Biomass And Wastes V, Lake Buena Vista, FL, Jan 26-30, 1981.

Geyer, W. A., "Growth, Yield, and Woody Biomass Characteristics of Seven Short-Rotation Hardwoods," Wood Sci., 13, 209-215 (1981).

Groenveld, M. R., "The co-current moving bed gasifier," Ph.D. Thesis, Twente University of Technology, Enschede, Neterlands, 1980.

Hallen, R. T., L. J. Sealock, and R. Cuello, "Influence of Alkali Carbonates on Biomass Volatilization," presented at the Fundamentals of Thermochemical Biomass Conversion Conference, Estes Park, CO, Oct 18-22, 1982.

Hatt, B. W., P. J. Iredale, G. A. Irlam, R. N. Shand, H. H. Sheena, and E. L. Smith, "Research on the Gasification of Biomass at the University of Aston in Birmingham," presented at the Fundamentals of Thermochemical Biomass Conversion Conference, Estes Park, CO, Oct 18-22, 1982.

Huffman, W. J., C. Lin, S. R. Beck, and J. E. Halligan, "Kinetic Analysis of Manure Pyrolizers," presented at the Technical Seminar: Thermochemical Conversion of Biomass Residues, Nov30-Dec1, Golden, CO, 1977.

Junge, D. C., "Boilers Fired with Wood and Bark Residues," Research Bulletin 17, Forest Research Laboratory, Oregon State University, Corvallis, OR, 1975.

Kunii. D., and O. Levenspiel, "Fluidization Engineering," Wiley, New York, 1969.

Maa, P. S., and R. C. Bailie, "Experimental Pyrolysis of Cellulosic Materials," presented at the AIChE 84th National Meeting, Atlanta, 1978.

Mingle, J. G., and R. W. Boubel, "Proximate Analysis of some Western Wood and Bark", Wood Sci., 1, 1 (1968).

Morgan, L. W., G. M. Armstrong, and H. C. Lewis, "Distillation of Hardwood in a Fluidized Bed," Chem. Eng. Prog., 49, 98-101 (1953).

Mullen, J. F., "Controlled Burning of Southern Pine Wood and Bark for Steam Generation," U. S. Department of Agriculture Forest Service Final Report FS 50, 3201-5.143, Southern Forest Experimental Station,Alexandria, LA, 1970.

Raman, K. P., W. P. Walawender, and L. T. Fan, "Gasification of Feedlot Manure in a Fluidized Bed Reactor. The Effect of Temperature," Ind. Eng. Chem. Proc. Des. Dev., 19, 623-629 (1980).

Raman, K. P., W. P. Walawender, L. T. Fan, and C. C. Chang, "Mathematical Model for the Fluid Bed Gasification of Biomass Materials. Application to Feedlot Manure," Ind. Eng. Chem. Process Des. Dev., 20, 686 (1981).

Rensfelt, E., B. Blomkvist, C. Ekstrom, S. Engstrom, B. G. Espenos, and L. Liinanki, "Basic Gasification studies for Development of Biomass Medium-BTU Gasification Processes," Symposium Papers, Energy from Biomass and Wastes, sponsored by IGT, Washington D. C., August 14-18, 1978.

Rose, G., and R. Zabransky, "Devolatilization of Maple Hardwood," presented at the Fundamentals of Thermochemical Biomass Conversion Conference, Estes Park, CO, Oct 18-22, 1982.

Schoeters, J., K. Maniatis, and A. Buekens, "Fuel Gas from Agricultural Residues in a Fluidized Bed Reactor," Proceedings 2nd World Congress of Chemical Engineering, 1, Montreal, Canada, Oct. 4-9, 1981.

Seamann, J. F., "Energy and Materials from Forest Biomass," Proc. Inst. of Gas Technol. Symp. on Clean Fuels from Biomass and Wastes, Orlando, FL Jan 25-28, 1977.

Singh, S. K., W. P. Walawender, L. T. Fan, and W. A. Geyer, "Steam gasification of Cottonwood (Branches) in a Fluidized Bed," Wood and Fiber Science, 18, 327-344 (1986).

Smil, V., "Biomass Energies," pp 80-81, Plenum Press, New York, 1983.

Soffer, S. S., and O. R. Zaborsky, "Biomass Conversion Processes for Energy and Fuels," p 20, Plenum Press, 1981.

Walawender, W. P., and L. T. Fan, "Gasification of Dried Feedlot Manure in a Fluidized Bed - Preliminary Pilot Plant Tests," presented at the 84th National Meeting, AIChE, Atlanta, Feb. 27, 1978.

Walawender, W. P., D. A. Hoveland, and L. T. Fan, "Steam Gasification of of Alpha Cellulose in a Fluid Bed Reactor," presented at the Fundamentals of Thermochemical Biomass Conversion Conference, Estes Park, CO, Oct 18-22, 1982.

Walawender, W. P., D. A. Hoveland, and L. T. Fan, "Steam Gasification of Pure Cellulose. Part I. Uniform Temperature Profile," Ind. Eng. Chem. Process Des. Dev., 24, 813-817 (1985a).

Walawender, W. P., M. A. Eriksson, D. S. Neogi, S. K. Singh, and L. T. Fan, "Effect of Steam To Feed Ratio on Biomass Gasification," presented at the Symposium on Gasification reactions of Carbonaceous Solids, AIChE meeting, Chicago, Nov 10-15, 1985b.

Yasihida, K., and D. Kunii, "Complex Reactions in Fluidized Bed-Simulation and Gasification," J.Chem. Eng. Japan, 7, 34-39 (1974).

Zerbe, J. I., and R. A. Anola, "Direct Combustion of Silvicultural Biomass," presented at the Symposium on Fuels from Biomass, Urbana, Apr. 19, 1977.

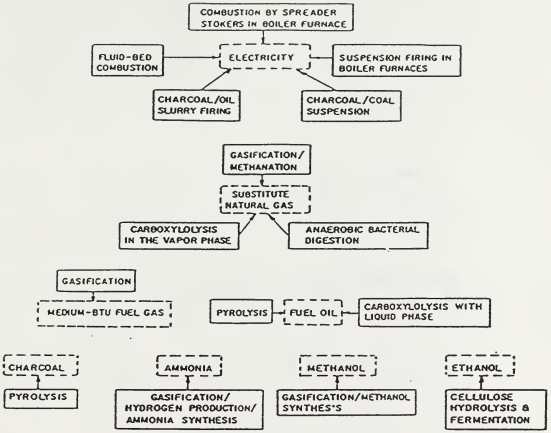

Figure 2.1. Conversion technologies for manufacturing wood-derived energy products. (Cheremisinoff, 1983).

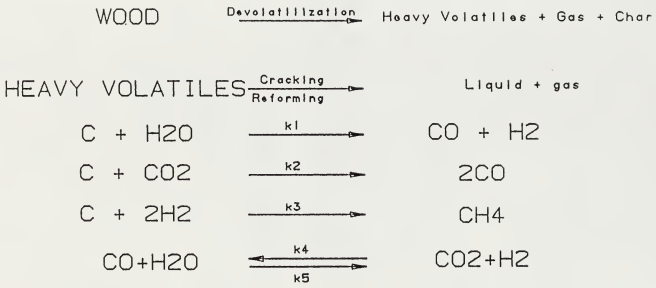

Figure 2.2. Reaction mechanism for gasification of wood.

CHAPTER 3

FLUIDIZED-BED GASIFICATION OF SIBERIAN ELM

Due to the depletion of fossil fuels, recent attention has been turned towards wood to supplement our future energy demands. Wood is an attractive energy resource, mainly because it can be produced, processed and utilized at lower costs compared to many of the conventional energy sources (Smil, 1983). A number of research efforts have been devoted to the efficient conversion of wood into energy and chemicals (Chow et al., 1983; Bailie, 1981). Currently, wood provides about 2% of our total energy demands and projected figures show that, by 1990, wood alone can contribute about 8% of the energy demand in the U. S. (Zerbe, 1981). In order to realize the vast potential of wood for energy, techniques such as short rotation intensive culture have been developed for the growth of woody plants with short harvest age (Geyer, 1981).

One method for the conversion of wood to fuel gas or synthesis gas is gasification. Gasification involves thermal decomposition (pyrolysis) at temperatures above 800 K coupled with secondary reactions of the volatiles. Pyrolysis alone results in appreciable char and tar production which complicates the process (Modell, 1982). Gasification has been found to increase carbon conversion through tar cracking, and the water-gas shift reaction. In steam gasification, control of the H2/CO ratio (important for the synthesis gas production) is facilitated. The influence of

major operating parameters such as temperature, particle size and gas residence time have been studied by various researchers.

Although the effect of steam-to-feed (S/F) ratio has been explored, its influence has not been determined conclusively. Antal (1978) concluded that S/F ratios up to 1.4 have little effect on the gasification of wood. Feldman (1981) also concluded that for a S/F ratio of 0.8, there is no net steam consumption. On the other hand, Rensfelt et al. (1978) concluded that steam is consumed through steam reforming reactions. Schoeters (1981) gasified wood with steam and explained their results through a water-gas shift reaction mechanism. Walawender et al. (1985a) explained their results for the steam gasification of cellulose through a water-gas shift reaction mechanism for temperatures above 940 K. Singh et al. (1986) reached the same conclusion for the steam-gasification of cottonwood. Similar results were obtained for Siberian elm gasification (Walawender, 1985b).

The principal objective of this chapter is to clarify the influences of steam and the S/F ratio on the product gas obtained from the steam gasification of wood in a fluidized bed. Systemmatic data were obtained for a S/F ratio range of 3 to 11 and statistically analyzed to asses the significance of this parameter.

EXPERIMENTAL FACILITIES AND PROCEDURE

Facilities

The overall system used in the present work is shown schematically in Figure 3.1. It consisted of three sections: the reactor, gas cleaning, and gas sampling sections. The reactor contained four zones: the disengaging, fluidized bed, packed bed, and gas inlet zones. The inlet, packed, and fluidized zones were constructed from a schedule 40 Inconel 600 pipe (I.D. 10.16 cm I.D. by 55 cm length); a second section of pipe (15.24 cm I.D. by 20 cm length) formed the disengaging zone (freeboard) of the reactor (see Figure 3.2). The bottom 25 cm of the reactor vessel served as the gas distribution and preheating zone. The top 15 cm of this section was packed with aluminium oxide pellets (0.5 cm in diameter). The packed bed section allowed the fluidizing gas to uniformly enter the fluidized-bed zone. The inlet zone and packed bed zones were separated by a 60 mesh 316 SS screen. The packed bed and fluidized bed were also separated by an identical screen. Instead of gaskets, heat resistant sealent was used between all flanges.

The bed was made up of a solid matrix containing 25% by weight of limestone and 75% by weight of silica sand; the limestone was added to prevent agglomeration which typically occurs in a bed composed only of silica sand (Walawender et al., 1981). The limestone particles ranged between -30 to

+50 mesh (0.59 mm to 0.287 mm). The static bed height was 8 to 10 cm, and the expanded bed height was 12 to 14 cm.

The reactor was heated by means of twelve quarter cylindrical electrical resistance heaters, each capable of delivering up to 1200 watts of power, with a maximum sustained operating temperature of 1550 K. The heaters were stacked in three tiers, each having four heaters. The top four quarter cylinder heaters were connected in parallel; the bottom two tiers had two parallel connections, each having two quarter-cylinders. Voltage to each set of heaters was controlled independently by PID controllers (Omega model 49K-814). There were five chromel-alumel thermocouples installed in the reactor. One of them, a sliding thermocouple, measured the axial temperature profile in the reactor. The others were located in the freeboard, fluidized-bed zone, preheating zone, and the middle of the reactor. The controllers indicated the temperatures measured by the thermocouples and activated the heaters as necessary to maintain a preset temperature profile inside the reactor. A pressure probe, connected to a water manometer, indicated the bed pressure and the state of fluidization.

The feed was introduced into the reactor by gravity flow through a vertical feed pipe (3 cm I.D.) which discharged at a location about 8 cm above the static bed. A Vibra Screw Feeder (Model SCR-20), with a solid core flight screw, delivered the feed material at a uniform volumetric

flow rate. A purge flow of nitrogen aided the flow of fine particles through the feed pipe and prevented gas backflow and subsequent condensation of vapor in the upper section of the feed pipe and the feeder.

Steam, produced externally in a Sussman Hot Shot electric boiler (Model MB-6), served as the fluidizing medium. It was supplied to the preheating section at a temperature of about 400 K and a pressure of about 200 kPa. A needle valve was placed in the steam line to control the steam flow rate.

The gas exiting from the reactor was passed through a cyclone to remove particulate solids (char). The reactor and cyclone were both insulated with Kao wool. The insulation maintained the cyclone at an elevated temperature to prevent condensation of steam. The gas stream leaving the cyclone was then passed through two water cooled single pipe heat exchangers placed in series. An additional glass condensor ensured complete condensation. A condensate receiver, at the exit of the exchangers, collected tar and steam condensate. The gas was further cleaned by means of a dry scrubber packed with glass wool. The scrubber effectively removed the fine tar mist from the gas without creating excessive pressure drop.

A wet test meter, connected to a strip chart recorder, measured the flow rate of gas as it discharged from the scrubber. A side draw of the gas stream was dried in a

column packed with drierite ($CaSO_4$) and then pumped to an on-line gas chromatograph for analysis.

Procedure

The heaters were turned on about three to four hours before the commencement of an experiment, and the controllers were set to the desired operating temperature. Air served as the feed pipe purge gas as well as the fluidizing agent during the heat-up period. Just before initiating an experiment, the steam generator was switched on; once steam was available, the fluidizing-air flow was gradually replaced by steam. A needle valve placed in the steam line adjusted the steam rate. The steam rate was measured by collecting the condensate downstream from the condensers.

When the gasifier reached the desired operating temperature, the axial temperature profile over the reactor and freeboard was measured with the sliding thermocouple, and the controllers were adjusted accordingly to maintain as uniform of an axial temperature profile as possible.

The feed rate was measured by disconnecting the lower section of the feed pipe and weighing the effluent collected over three-minute time intervals. This was done three times at the start and end of each run, respectively, to ensure uniform feeding throughout the experiment. When the feeding started the temperature of the reactor dropped slightly but

it was adjusted to the set point by the controllers. A gas sample was extracted about 10 minutes after the initiation of feeding, and every 11 minutes thereafter by an automatic sampler on the gas chromatograph. The flow rates of condensate and nitrogen were measured at regular intervals throughout the run. A typical run lasted 100 to 120 minutes; the data obtained in the last 40 to 50 minutes were used for analysis.

It was impossible to measure the total char produced in a run because of the hold-up of char in the bed. It was also impossible to measure total tar due to hold-up in the heat exchangers.

Chemical Analysis

The dry off-gas was analyzed with an Applied Automation (Optichrom 2100) on-line process gas chromatograph. The components of interest were H_2, CO, CO_2, CH_4, C_2H_4, C_2H_6, C_3H_6, C_3H_8, O_2, and N_2. The chromatograph had a cycle time of 11 minutes. Moisture and ash in the feed and char were analyzed according to the standard ASTM procedures in a ventilated oven and muffle furnace, respectively. Elemental analyses of the feed, and char were conducted with a Perkin-Elmer (model 240B) elemental analyzer. The heat of combustion of the wood was measured with a bomb calorimeter.

Operating Conditions

The ranges of the operating conditions for all the runs are summarized in Table 3.1. The axial temperature profile was maintained as uniform as possible in each run. Steam and feed rates were simultaneously adjusted to give the desired steam-to-feed (S/F) ratio while maintaining a uniform gas residence time in the reactor. In maintaining the gas residence time constant, it was necessary to vary the steam rate according to the operating temperature. The gas residence time varied between 4 and 6.5 seconds; it was estimated on the basis of the reactor temperature, total dry gas flow rate and steam rate.

Feed Material

Siberian Elm (Ulmus pumila L.), a medium density wood of specific gravity 0.46 was the feed material. Ten trees planted on an upland silt loam prairie soil were randomly selected and were chipped in their entirety with a Mobark chipper. The chips were isolated from the branches and air dried. They were then ground in a hammer mill. The ground material was then sieved to remove the -28 to + 50 mesh fraction which served as the feed material. The particle size was further reduced by passing the sieved fractions through a Fritz mill with a 0.020 in (0.508 in) screen. The elemental analysis of the feed material is presented in Table 3.2.

METHOD OF DATA ANALYSIS

The necessary calculations were executed with the data obtained during the last 40-50 minutes of each run, when the reactor was operating under steady-state conditions. Each gas chromatograph (GC) cycle in the steady-state period was treated as an individual data point. For each data point, the axial temperature profile was measured, and the average of the temperature measurements was taken as the representative temperature for the data point. Again, for each data point, the gas flow rate was measured separately. The GC readings were adjusted for the nitrogen purge to determine the dry product gas composition.

The gas higher heating value (HHV) (on a volumetric basis) was calculated from the composition of the dry gas and the standard heat of combustion of each component . The volumetric flow rate of the product gas was determined from the difference in the rates measured by the wet test meter with and without feeding. The volumetric gas yield per unit mass of feed (on a dry ash-free basis (DAF)) was calculated from the volume flow rate of the dry produced gas (at 288 K and 101.3 kPa) and the mass rate of the DAF.

The energy recovery (expressed as percentage) was calculated from the ratio of the product of the gas yield per unit mass of DAF feed and the HHV of gas to the heat of combustion of a unit mass of DAF feed. It represents the percentage of the energy content of the feed that is present

as combustible gas. The carbon conversion (again expressed as percentage) was determined from the ratio of the atoms of carbon in the gas produced from a unit mass of DAF feed to the atoms of carbon in a unit mass of DAF feed. It represents the percentage of carbon in the feed converted to gas. The mass yield of gas was evaluated by converting the volumetric yield to a mass basis.

STATISTICAL ANALYSIS

The experiments were designed to investigate the effects of temperature and S/F ratio on the gasification characteristics. The combinations of temperature and S/F ratio studied are presented in matrix form in Table 3.3. The order in which the experiments were conducted was randomized to reduce bias. All the statistical analyses were conducted with the SAS (Statistical Analysis System, Version 5) package.

Single Variable Regression

Regression analyses are performed to determine the "best-fit" polynomial relationships between the independent variable and the dependent variables, (e.g. gas volumetric yield vs temperature for a fixed S/F ratio). An analysis of variance is performed to test the significance of each regression model. The coefficients determined from the regression analyses are accepted as being significant or

rejected on the basis of the F-test statistic at the 5% significance level. The criteria for selecting the "best fit" model include F-test, parameter significance level, and the R-square values.

In order to determine if there is a significant effect of a parameter on a particular dependent variable (e.g S/F ratio on each gasification characteristic), the single varaible regression models are compared with the "General Linear Test Approach" (Neter and Wasserman, 1974). In this approach, the regression model coefficients are compared for different values of the parameter studied with the F-test as the decision criteria for models of the same order.

Multi-Variable Approach

Regression models with more than one independent variable (e.g. temperature and S/F ratio) are examined. Additionally, interaction terms between the independent variables are also considered in the model. This analysis employs three methods for selecting the best regression model; (1) Forward Selection, (2) Backward Elimination, and (3) Maximum R-Square Improvement. The criteria for selecting the best model are the F-test, parameter significance level, R-square value and C(P) value (see, e.g., Ott, 1984). A model is chosen to have all variables significant if the C(P) value is approximately equal to the number of variables in the model.

In the present work, temperature and the S/F ratio constitute the independent variables. Hence, the form of the regression model is as follows

$$y = A + BT + CT^2 + DS + ES^2 + F\ T*S$$

where

y response variable

A coefficient of the zero order term

B,D coefficients of the first order terms in temperature and steam-to-feed ratio respectively

C,E coefficients of the second order terms in temperature and steam-to-feed ratio respectively

F coefficient of the interaction term

T temperature of the reactor in K

and

S S/F ratio

RESULTS

The experimental data for Siberian elm gasification were divided into three groups, according to the S/F ratio employed in the experiments (S/F = 3, 7 and 11), for the single variable regression analyses. Each group was separately analyzed to establish the relationship between

temperature and the various gasification characteristics. The major characteristics of interest were the compositions of the major components of the dry product gas, the dry gas heating value, the volumetric and mass yields of the dry product gas, the carbon conversion to gas, and the energy recovery.

The effects of temperature on the gasification characteristics for various S/F ratios are illustrated in Figures 3.3 through 3.10. In all the figures, the lines represent the selected regression models. The regression coefficients for the "best-fit" relationships between temperature and the gasification characteristics are summarized in Table 3.4.

Statistical comparisons of the regression models with temperature as the independent variable were attempted to assess the effect of S/F ratio on the gasification characteristics. When the orders of the regression models being compared were not the same at different S/F ratios, they were forced to be the same (generally higher order was reduced to first order) thereby enabling comparisons. It was not possible to compare all of the gasification characteristics due to differences in variances. Comparisons were possible only for the concentrations of CO and CO_2, the mass yield of gas and the energy recovery. The results of these comparisons are summarized in Table 3.5.

For the multi-variable regression, both the S/F ratio and temperature were the independent variables. The results of this analysis are presented in Table 3.6. Figure 3.11 compares multi-variable regression models for H_2 and CO for S/F ratios of 3 and 11. The models for mass yield of gas and volumetric yield of gas at S/F ratios of 3 and 11 are compared in Figure 3.12. Carbon conversions and energy recoveries are presented in Figure 3.13.

DISCUSSION

Biomass gasification has been studied in detail by Antal et al. (1978) and others. Most researchers agree that, conceptually, gasification occurs in three stages, (1) Pyrolysis or devolatilization which produces volatile matter and char, (2) secondary reactions of the volatiles and (3) gasification of char by steam.

Thermogravimetry of wood and other biomass has shown that the majority of devolatilization takes place over a 300 K temperature interval and that it is essentially complete at a temperature of 800 K. The rate of biomass devolatilization has been investigated by Raman et al. (1981a, 1981b) and Antal (1978,1979). Antal (1979) has calculated that the time for completion of devolatilization of small biomass particles (75-250 microns in size) to be less than 0.5 sec. Devolatilization in a fluidized-bed reactor has been found to be nearly instantaneous for small particles (Raman et al., 1981a). Char yields for fast pyrolysis of small wood particles in a fluidized bed have been determined to be less than 10% (van den Aarsen et al., 1982). Consequently, for fluidized-bed gasification, only steps 2 and 3 of the conceptual gasification mechanism need to be of concern.

Antal (1979) has indicated that the secondary gas phase reactions (tar cracking and the water-gas shift reaction) are important in determining the gas composition. He has

stated that the important factors are temperature and the gas phase residence time (ie. the time-temperature history of the volatiles).

Walawender et al. (1982) have hypothesized that in the case of the gasification of alpha cellulose, the secondary reactions can be divided into two regimes: a tar cracking dominated regime (for T < 940 K) and a water-gas shift reaction dominated regime (for T > 940 K). Assuming that the water-gas shift reaction was the sole reaction for temperatures above 940 K, Walawender et al. (1982) have related the slope of the gas yield-temperature plot, to the slopes of the mole fraction-temperature plots of the components (H_2, CO_2, and CO) over this temperature regime. They also have demonstrated that the slopes for CO, CO_2 and H_2 are approximately in the proportions -1:1:1. These proportions are required by the water-gas shift reaction stoichiometry;

$$CO + H_2O \longrightarrow CO_2 + H_2$$

Singh et al. (1986) have found a similar behavior for the gasification of cottonwood. In the second temperature regime, they were able to force-fit their gas composition data to the -1:1:1 proportions with a maximum deviation of 2.5 %. Unlike cellulose, they observed that the carbon conversion continued to increase for temperatures greater than 940 K; this was attributed to the cracking of tars

originating from lignin. Nevertheless, they concluded that the water-gas shift was the dominant secondary reaction above 940 K.

Rensfelt et al. (1978) and Antal (1978) have indicated that gasification of char is not significant for temperature ranges typical of this work. However, they were concerned with relatively low S/F ratios (i.e.<1). In the present work, the S/F ratio was sometimes greater than 10, providing a high driving force for the steam gasification of char. This point will be elaborated on later.

In the present set of experiments, the time-temperature history variations of the volatiles were minimized. Moreover, since most experiments were conducted above 940 K, the results can be explained primarily in terms of the water-gas shift reaction. Analysis of the systemmatic data obtained in this work provided a variety of evidences to further support the contention of dominance of the shift reaction. These evidences are presented in the following paragraphs.

Evidence for Water-gas Shift Reaction

The variations in the compositions of the major components of the dry product gas with temperature are shown in Figures 3.3 through 3.5 with S/F ratio as a parameter. The sum of the concentrations of CO and CO_2 in the dry product gas have been found to decrease with temperature at

each S/F ratio for temperatures above 940 K. Additionally, straight lines of a common (absolute) slope, force-fitted to the experimental plots for the concentrations of CO, CO_2 and H_2 with the CO plot as the basis, indicate that in the case of H_2, the maximum deviations of these fits from the data are 2.5%, 0.5% and 1.5% (for S/F = 3,7 and 11 respectively). In the case of CO_2 the deviations have been found to be less than 10%. These findings are consistent with the dominance of the water-gas shift reaction.

If it is assumed that water-gas shift reaction is the only secondary gas phase reaction, then according to the stoichiometry, the sum of the number of moles of CO and CO_2 must be constant for any temperature. Also, the increase in the number of moles of H_2 is equal to the decrease in the number of moles of CO and their sum is constant. Thus, based on the stoichiometry, we can write

$$\left[\frac{n_{CO} + n_{CO_2}}{n_{CO} + n_{CO_2}} \right] = \text{constant} = A$$

The variations due to different feed rates is normalized by the above ratio. The number of moles of each species are calculated from the gas concentrations and the gas volumetric flow rate (on dry basis). A plot of A vs. temperature is shown in Figure 3.14. From the plot it is clearly seen that for temperatures above 940 K, the ratio A

does not vary appreciably. It should be noted that the points on the graph cover the range of experimental S/F ratios.

The gas higher heating values obtained in the present experiments also show consistency with the hypothesis of a water-gas shift reaction dominated zone. In this regime, the gas heating value should decrease slightly with an increase in temperature due to the diluent effect of CO_2 which was what was observed. Also, the increases in the dry gas volumetric and mass yields are consistent with the water-gas shift hypothesis. In the temperature region above 940 K, mass yields greater than 1 kg gas/kg DAF feed have been obtained. This result is a direct consequence of the shift reaction.

Though the condensate rates could not be measured with sufficient accuracy to precisely determine the amount of steam consumption, it was generally observed that the condensate rate dropped after the feed started in all the experiments. Also the amount of reduction increased with increasing temperature.

The carbon conversion has been observed to continue to increase with temperature for temperatures above 940 K as illustrated in Figure 3.10. This may be due in part to the fact that although lignin tar cracking is not complete at 940 K, it may be small enough to not mask the dominance of the water-gas shift reaction (Singh, 1986). Due to the high

S/F ratios employed, char gasification may be partially responsible for the increase in the carbon conversion. Evidence for steam gasification of char is presented later.

Effect of Steam-to-Feed Ratio

The preceeding discussion implies that the water-gas shift reaction is the dominant reaction above 940 K when steam is present in large excess. One of the major objectives of this work was to determine the effect of the S/F ratio on the gasification characteristics. The effect of the S/F ratio on the gasification process has not been previously studied in a systematic fashion.

The statistical approach suggested by Neter-Wasserman (1974) was employed in an attempt to determine the effect of the S/F ratio on the gasification characteristics. However, differences in the order of the regression models and differences in the variances for different S/F ratios did not allow statistical comparisons to be made for all the characteristics. Comparisons were only possible for the concetrations of CO and CO_2, the energy recovery, and the mass gas yield.

Since the method of Neter-Wasserman was not fruitful, a two variable regression was employed for analyzing the effect of the S/F ratio. The multiple regression models, plotted in Figures 3.11-3.13, reveal the effects of S/F ratio and temperature on the gasification characteristics.

The curves have been plotted by substituting values of 3 and 11 in the regression models given in Table 3.6.

Figure 3.11 shows a decrease in concentration of CO and an increase in that of H_2 with an increase in the S/F ratio; this is what we would expect from the water-gas shift reaction hypothesis. Also, an increase in the S/F ratio results in increase in gas mass and volumetric yields (Figure 3.12) and increase in energy recovery (Figure 3.13). Increasing the S/F ratio provides an increase in the driving force for the water-gas shift reaction; this results in an increase in the amount of steam converted to product gas and subsequently larger mass and volumetric gas yields.

Higher heating values of the gas do not vary appreciably with S/F ratios. However, an increase in the S/F ratio results in an increase in the energy recovery through the increase in the volumetric gas yield.

We also note an increase in the carbon conversion with increaing S/F ratio (Figure 3.13), which can not be explained on the basis of water-gas shift reaction. Since tar cracking is influenced primarily by temperature, the increase in the carbon conversion with an increase in the S/F ratio can only be attributed to steam gasification of char.

From the above discussion, we infer that S/F ratio is an important parameter in the determination of gasification characteristics for a S/F ratio range of 3 to 11.

In closing, it is appropriate to comment on the approach to equilibrium in the gas phase. The ratio of the experimental mole fractions $y_{CO2} \cdot y_{H2} / y_{CO} \cdot y_{H2O}$, (assuming ideal gas behavior) has been plotted against temperature for a S/F ratio of 7 in Figure 3.15. This ratio is calculated on a wet gas basis from the dry gas volumetric flow rate, the dry gas composition and the steam flow rate. It is compared with the equilibrium constant, K, where

$$K = \frac{y^*_{CO2} \cdot y^*_{H2}}{y^*_{H2O} \cdot y^*_{CO}} ,$$

the starred quantities represent the equilibrium concentrations of the respective gaseous species. As can be seen from Figure 3.15, the experimental data points are significantly offset from equilibrium (solid curve) at low temperatures and only tend to approach equilibrium at higher temperatures.

By slightly altering the experimental mole fraction ratio it is possible to construct a plot of

$$\frac{y_{CO2} \cdot y_{H2}}{y^2_{CO}} \quad \text{vs} \quad \frac{y_{H2O}}{y_{CO}}$$

as shown in Figure 3.16. This plot reflects a variable S/F for a given T. The solid line represents equilibrium condition for a temperature of 1073 K. From the figure, it can be seen that there is an apparent correlation of the data at each temperature over the range of S/F ratio.

CONCLUDING REMARKS

The observed behavior of the steam gasification characteristics of Siberain elm are consistent with the conceptual mechanism proposed by Walawender et al. (1982): at temperatures above 940 K the process is dominated by the water-gas shift reaction. Moreover, steam, when in present in large excess, takes an active part in the gasification, being converted to product gas in significant amounts.

Multilple regression models for the gasification characteristics indicate that an increase in the S/F ratio results in increases in the concentrations of H_2 and CO_2, a decrease in the concentration of CO, increases in the volumetric and mass yields of gas, and increase in the energy recovery. All these can be explained by the shift reaction postulation. The observed increase in the carbon conversion can be attributed to the steam gasification of char.

While steam is an active gasification agent for the range of S/F ratio studied, the gas phase is not in equilibrium.

REFERENCES

Antal, M. J., W. E. Edwards, H. L. Friedman, and F. E. Rogers, "A Study of the Steam Gasification of Organic Wastes," Project Report to EPA, W. W. Liberick, Project Officer, 1978.

Antal, M. J., "The Effects of Residence Time, Temperature, and Pressure on the Steam Gasification of Biomass", presented at the Symposium on Biomass as a Non-Fossil Fuel Source, Div. of Fuel Chem. ACS meeting, Honolulu, Apr 1-6, 1979.

Bailie, R. C., "Results from Commercial-Demonstration Pyrolysis Facilities (35-45 tons/day refuse) Extended to Producing Synfuels from Biomass," Symposium papers, Energy from Biomass and Wastes V, sponsored by IGT, Lake Buena Vista, Florida, Jan 26-30, 1981.

Chow, P., G. L. Rolfe, and L. E. Arnold, "Chemicals, Fiber, and Energy from Woody Biomass," Illinois Research Notes, pp 11-13, 1985.

Modell, M., "Gasification and Liquefaction of Forest Products in Supercritical Water," presented at the Fundamentals of Thermochemical Biomass Conversion Conference, Estes Park, CO, Oct. 18 - 22, 1982.

Neter, J., and W. Wasserman, "Topics in regression Analysis" in "Applied Linear Statistical Models," pp 160-165, Richard D. Irwin, London, 1974.

Ott, L., "An Introduction to Statistical Methods and Data Analysis," 2nd Edition, pp 459-493, Duxbury Press, Boston, 1984.

Raman, K P., W. P. Walawender, L. T. Fan, and J. A. Howell, "Thermogravimetric Analysis of Biomass Devolatilization Studies on Feedlot Manure," Ind. Eng. Chem. Proc. Des. Dev., 20, 630-636 (1981 a).

Raman, K. P., W. P. Walawender, L. T. Fan, and C. C. Chang, "Mathematical Model for Fluidized Bed Gasification of Biomass Materials. Application to Feedlot Manure," Ind. Eng. Chem. Proc. Des. Dev 20 , 686-692 (1981 b).

Rensfelt, E., G. Blomkvist, C. Ekstrom, S. Engstrom, B. G. Espenos, L. Liinanki, "Basic Gasification Studies for Development of Biomass Medium BTU Gasification Processes," Symposium Papers on Energy from Biomass and Wastes (Washington, D.C : Institute of Gas Technology), pp 465-494, August 14-18, 1978.

Schoeters, J., K. Maniatis, and Buekens, "Fuel gas from Agricultural Residues in a Fluidized Bed Reactor," pp 313-317, Proceedings of the 2nd World Congress of Chemical engineering, Vol. I, Montreal, Canada, Oct.4-9, 1981.

Singh, S. K., W. P. Walawender, L. T. Fan, and W. A. Geyer, "Steam Gasification of Cottonwood (Branches) in a Fluidized Bed," Wood and Fiber Science, 18, 327-344, (1986).

Smil, V., "Biomass Energies," pp 80-81, Plenum Press, New York, 1983.

van den Aarsen, F. G., A. A. C. M. Beenackers, and W. P. M. van Swaaij, "Wood Pyrolysis and Carbon Dioxide Char Gasification in a Fluidized Bed," presented at the Fundamentals of Thermochemical Biomass Conversion Conference, Estes Park, CO, Oct. 18-22, 1982.

Walawender, W. P., S. Ganesan, and L. T. Fan, "Steam Gasification of Manure in a Fluidized Bed, Influence of Limestone as a Bed Additive," presented at IGT Symposium on Energy from Biomass and Wastes V, Lake Buena Vista, FL, Jan. 26-30, 1981.

Walawender, W. P., D. A. Hoveland, and L. T. Fan, "Steam Gasification of Alpha-Cellulose in a Fluidized Bed Reactor," presented at the Fundamentals of Thermochemical Biomass Conversion Conference, Estes Park, CO, Oct. 18-22, 1982.

Walawender, W. P., D. A. Hoveland,and L. T. Fan, "Steam Gasification of Pure Cellulose. Part I, Uniform Temperature Profile," Ind. Eng. Chem. Process. Des. Dev., 24, 813-817 (1985 a).

Walawender, W. P., M. A. Eriksson, D. Neogi, S. K. Singh, and L. T. Fan, "Effect of Steam-to-Feed Ratio on Biomass Gasification," presented at the 1985 AIChE Annual Meeting , Chicago, Nov. 10-15, 1985 b.

Zerbe, J. J., "The contribution of wood to the energy picture", presented at Conference on Wood- An Alternate Energy Resource for Appalachian Industry and Institutions, Proceedings published by School of Engg., North Carolina State University, 1981.

Table 3.1. Reactor Operating Parameters.

Reactor Temperature Range (K)	850 - 1125
Fluidizing Gas	Steam
Superficial Velocity (m/sec)	0.14 - 0.165
Condensate Rate (cc/min)	9.0 - 17
Feed Rate (DAF gm/min)	0.9 - 4.0
Steam-to-Feed Ratio	3 - 11

Table 3.2. Analysis of Siberian elm.

Ultimate Analysis (% dry basis)	Mean	Std.Deviation
Ash	1.70	0.41
C	47.11	0.47
H	5.73	0.08
N	0.33	0.13
O[1]	45.13	0.62
Moisture Content	5.43	0.09
Empirical Formula	$C_6H_{8.8}O_{4.3}$	
Heat of Combustion (DAF basis)*	18.12 (MJ/m^3)	

[1] by difference
* measured

Table 3.3. Operating Temperatures and Steam-to Feed Ratios.

Temperature,K / Steam-to-feed ratio	875	925	975	1060	1100
3		x	x	x	x
6		x	x	x	x
7	x	x	x	x	x
10	x	x	x	x	
11	x	x	x	x	x

x represents that experiments were done at this temperature and steam-to-feed ratio.

Table 3.4. Statistical Analysis of the Siberian elm Gasification Results.

Dependent variable	steam-to-feed Ratio	R^2	Significant Regression Model $y = A + BT + CT^2$		
			A	B	C
mole % H_2	3	0.97	-65.221	0.1036	
	7	0.93	-57.747	0.1059	
	11	0.98	-318.02	0.6737	-0.0003056
mole % CO	3	0.98	112.34	-0.0893	0
	7	0.99	492.83	-0.8711	0.0003899
	11	0.95	365.70	-0.6350	0.0002821
mole % CO_2	3	0.93	200.73	-0.3660	0.0001914
	7	0.86	- 92.11	0.2251	-0.0001034
	11	0.86	-287.26	0.6116	-0.0002914

Table 3.4. Statistical Analysis of the Siberian elm Gasification Results. (contd.)

Dependent variable	steam-to-feed Ratio	R^2	Significant Regression Model $Y = A + BT + CT^2$		
			A	B	C
Gas Yield (m^3/kg DAF feed)	3	0.94	-3.5872	0.0045	
	7	0.92	-2.8609	0.0039	
	11	0.82	-3.0649	0.0043	
	11	0.86	-13.8942	0.02658	0.000011546
Mass Yield (Kg/Kg DAF feed)	3	0.89	-2.5350	0.0034	
	7	0.90	-2.0164	0.0029	
	11	0.85	-2.2612	0.0033	
	11	0.88	-17.4148	0.03286	-0.000014104
Carbon Conversion (%)	3	0.79	-127.70	0.1856	
	7	0.91	-128.96	0.1922	
	11	0.85	-1005.69	1.9631	-0.0008816
Energy Recovery (%)	3	0.90	-1544.6	2.9803	-0.0013710
	7	0.89	- 923.5	1.7821	-0.0007818
	11	0.85	-1208.2	2.3353	-0.0010432

Table 3.5. Results of the Statisticsl Tests.

Dependent variable	R^2 3	7	11	3,7	Comparison 3,11	Results 7,11
I order CO	0.98	0.93	0.85	NP	NP	diff
IIorder CO	0.97	0.99	0.95	diff	diff	diff
II order CO_2	0.93	-	0,86	NP	diff	NP
I order energy	0.80	0.85	0.76	diff	diff	diff
IIorder energy	0.90	0.89	0.85	diff	diff	diff
I order mass	0.89	0.90	0.87	not diff	diff	diff
I order gas	0.94	0.92	0.82	diff	NP	NP

- means the order of regression is not valid
NP means the comparison is not possible
diff means the regression lines are significantly different
not diff means the regression lines are not different

Table 3.6. Two Parameter Analysis. ($y = A+BT+CT^2+DS+ES^2+F\ S*T$)

Dependent Variable y	A	B	C	D	E	F
Mole% CO	494.39	-0.800	0.000338	-8.87492	0.2863	0.00391
Mole% CO_2	-57.64	0.148	-0.000063	0.00016	0	0
Mole% H_2	-312.07	0.529	-0.000191	13.99461	-0.3627	-0.00805
Gas Yield	-3.566	0.004	0	0	0.0019	0
Energy Recovery	-641.08	1.151	-0.000453	1.62691	0	0
Mass Yield	-2.136	0.0031	0	-0.61	0.0054	0
Carbon conversion	-98.124	0.1702		-6.0229	0.4864	

Sample size 109
T represents temperature in K
S represents steam-to-feed ratio

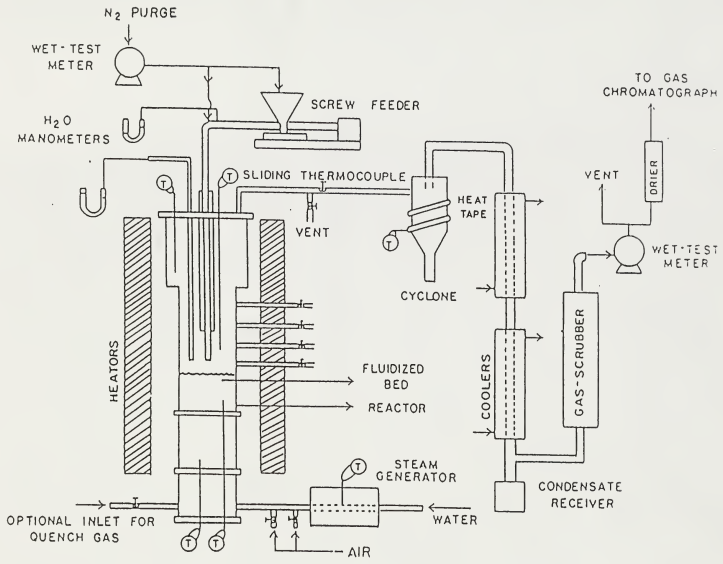

Figure 3.1. Bench-Scale fluidized-bed wood gasification system.

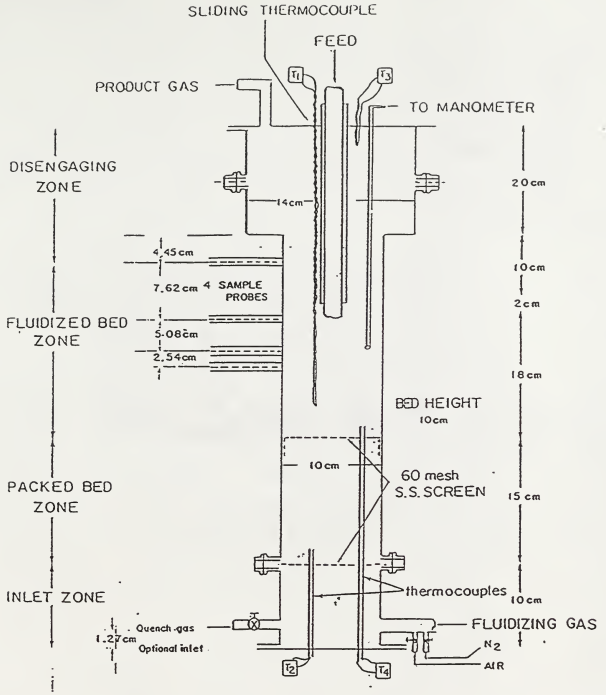

Figure 3.2. Fluidized bed reactor.

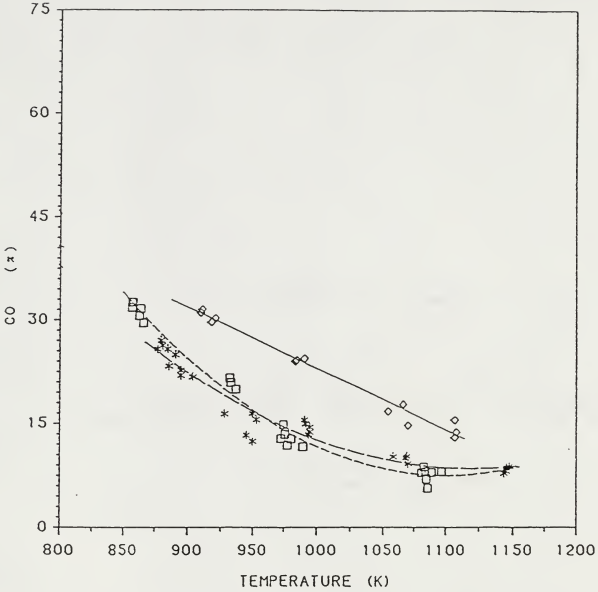

Figure 3.3. Concentration of CO in the product gas with different steam-to-feed ratios. —◇— represents S/F ratio of 3 —□— —□—represents S/F ratio of 7 and—+— —*—represents S/F ratio of 11.

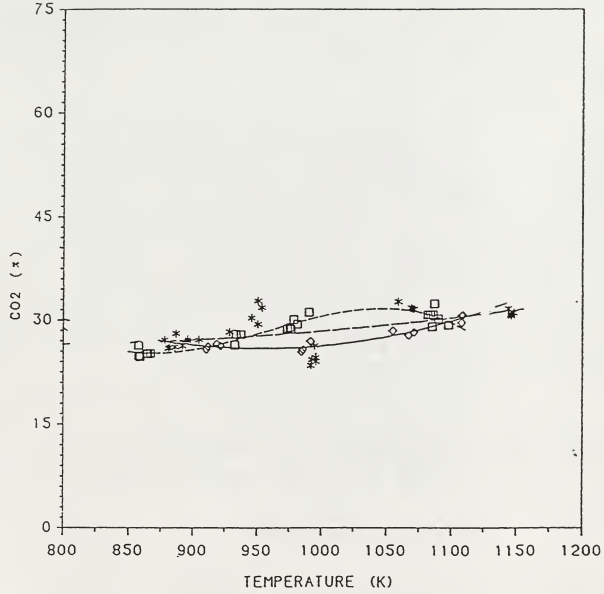

Figure 3.4. Concentration of CO_2 in the product gas with different steam-to-feed ratios. —◇—◇— represents S/F ratio of 3 —□—□— represents S/F ratio of 7 and —✳—✳— represents S/F ratio of 11.

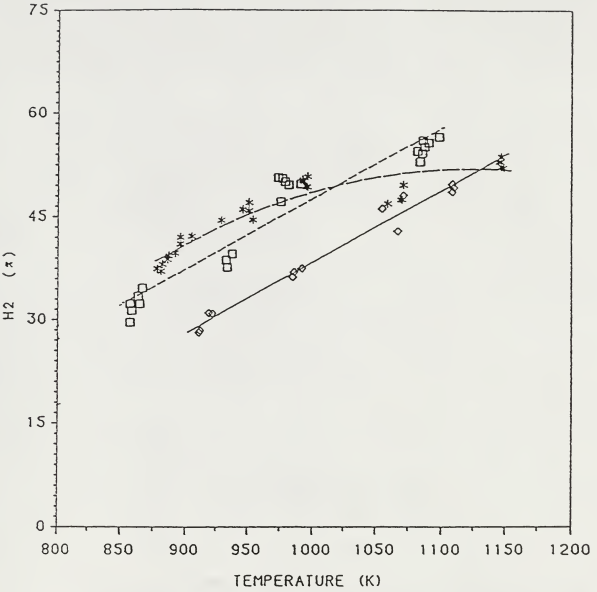

Figure 3.5. Concentration of H_2 in the product gas with different steam-to-feed ratios. ◇-◇ represents S/F ratio of 3, □-□ represents S/F ratio of 11 *-* represents S/F ratio of 11.

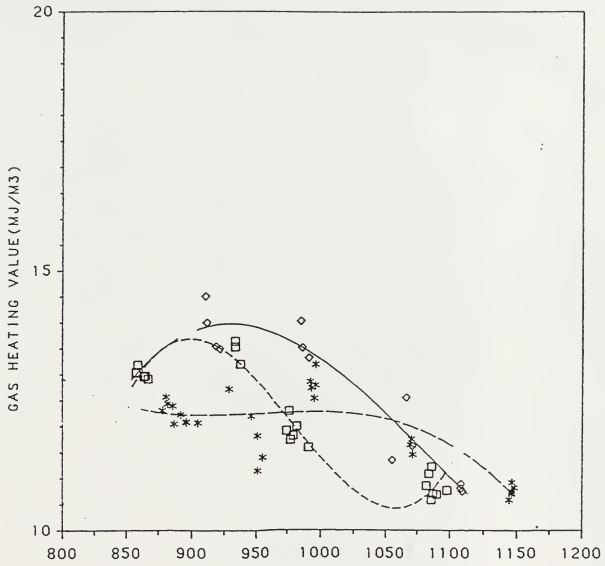

Figure 3.6. Higher heating value of gas with different steam-to-feed ratios. —◇—◇— represents S/F ratio of 3, — □ — □ represents S/F ratio of 7 and —✳— —✳— represents S/F ratio of 11.

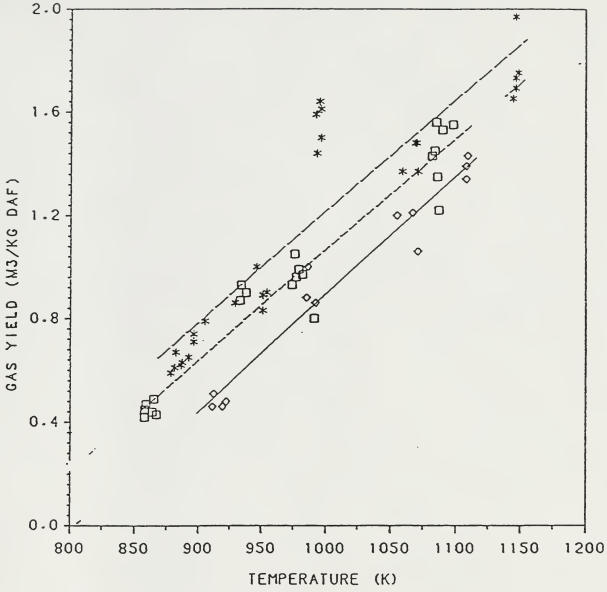

Figure 3.7. Volumetric gas yield vs temperature with different steam-to-feed ratios. ◇—◇—◇ represents S/F ratio of 3, -□- ⊟ - -represents S/F ratio of 7, —*— —*— represents S/F ratio of 11.

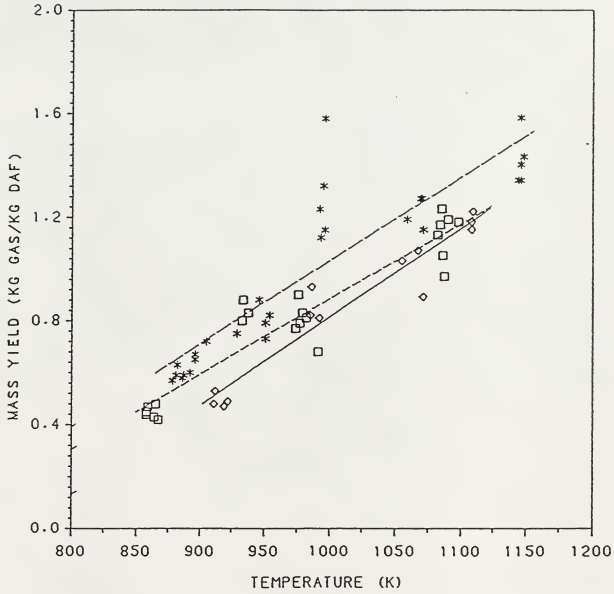

Figure 3.8. Gas mass yield vs temperature with different steam-to-feed ratios. —◇—◇— represents S/F ratio of 3, ⊟ – ⊟ represents S/F ratio of 7 and —*—*— represents S/F ratio of 11.

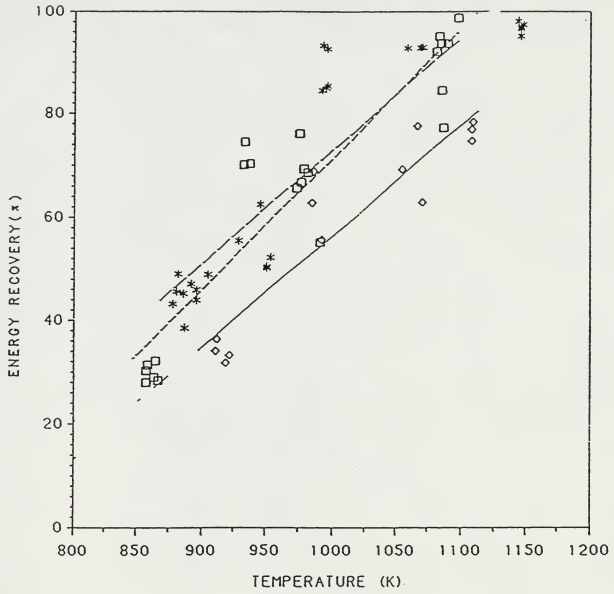

Figure 3.9. Energy recovery vs temperature with different S/F ratios. ◇——◇——◇ represents S/F ratio of 3, □ — □ — □ represents S/F ratio of 7 and ✳— —✳— —✳ represents S/F ratio of 11.

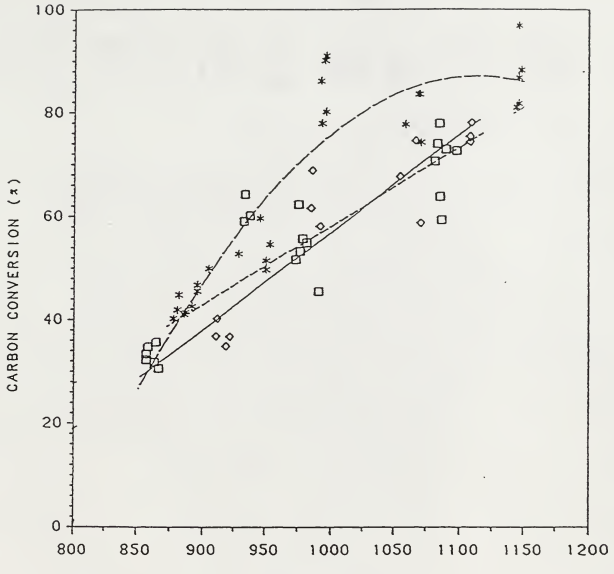

Figure 3.10. Carbon conversion vs temperature with different S/F ratios. -◇-◇-◇- represents S/F ratio of 3, ⊟-⊟-⊟represents S/F ratio of 7 and *-*-*-* represents S/F ratio of 11.

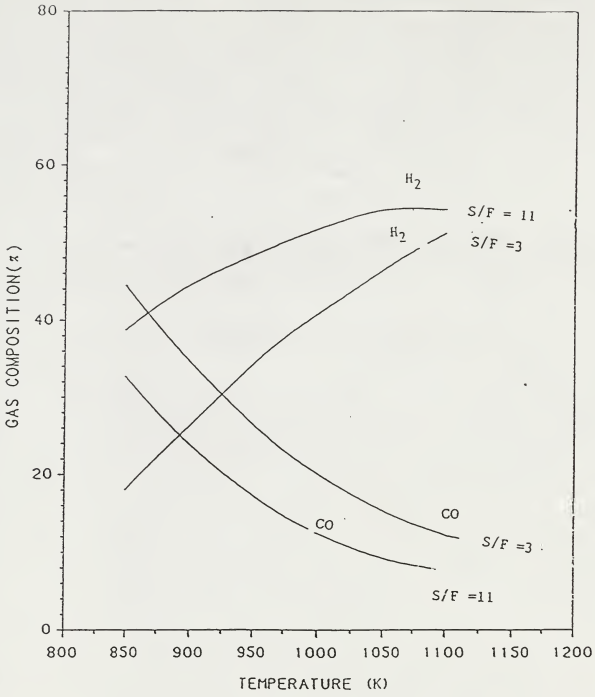

Figure 3.11. Effect of temperature and steam-to-feed ratio on gas composition.

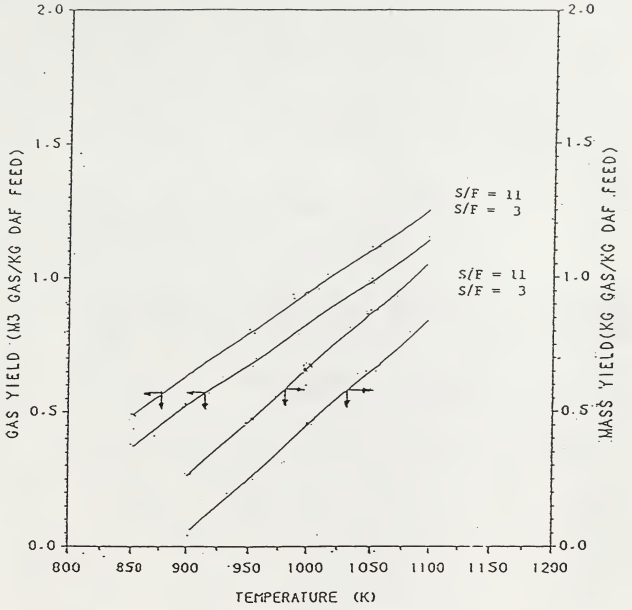

Figure 3.12. Effect of temperature and steam-to-feed ratio on gas volumetric and mass yields.

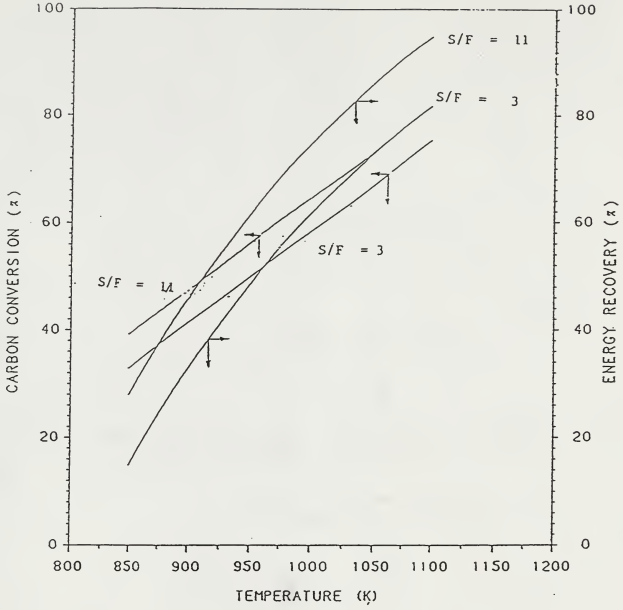

Figure 3.13. Effect of temperature and steam-to-feed ratio on carbon conversion and energy recovery.

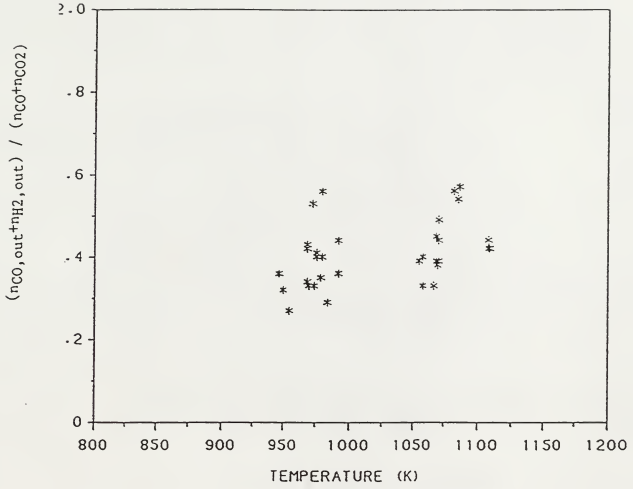

Figure 3.14. Reactor $(n_{CO,out}+n_{H2.out})/(n_{CO}+n_{CO2})$ vs temperature.

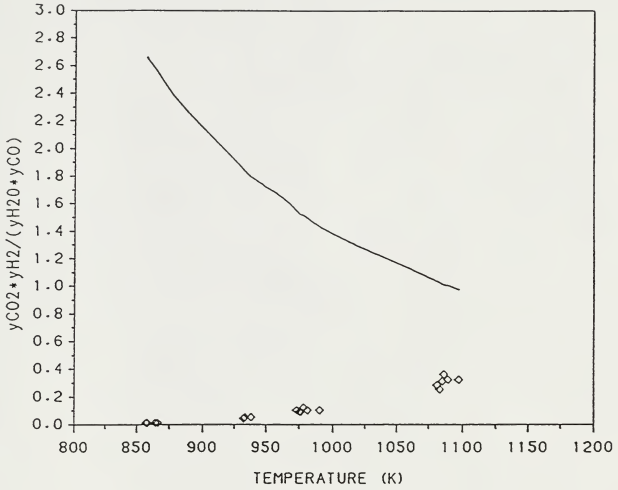

Figure 3.15. Reactor mole fraction ratio (yCO_2*yH_2) / (yH_2O*yCO) vs temperature with a steam-to-feed ratio of 7.

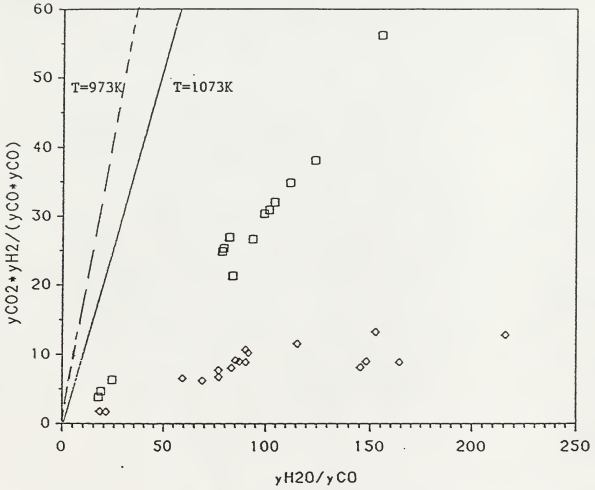

Figure 3.16. Reactor mole fraction ratio(yCO_2 * yH_2)/(yCO*yCO) vs yH_2O/yCO ratio for different temperatures. ◇ represents temperatures of 973 K and □ represents temperatures of 1073 K.

CHAPTER 4

MATHEMATICAL MODELING OF FLUIDIZED-BED GASIFICATION

In recent years, the gasification of wood in fluidized beds has received increasing attention. Low and medium Btu fuel gas and synthesis gases have been the products of interest. In addition to experimental studies, mathematical modeling efforts have been conducted to aid in scale-up, design and process control. The modeling efforts vary considerably in their sophistication; they range from early simple models based only on char gasification to more recent models which attempt to include devolatilization. All of the models to date have been based on isothermal conditions and have only considered the bed section.

Some of the proposed models have been based on the two phase theory of fluidization. They employ either the Kunii and Levenspiel model (K-L) (1969) or the Davidson and Harrison model (D-H) (1971). Yoshida and Kunii (1974) have modeled the gasification of pure carbon with air or steam based on the K-L two-phase theory. The model assumes water-gas shift reaction equilibrium and pseudo-first order kinetics for the char gasification reactions. The char gasification reactions include the reactions of char with O_2, CO_2 and steam. The model only considers the reactions in the bed section. They have compared their simulated results with experimentally determined compositions; reasonable agreement has been obtained by adjustment of system parameters. Their model has the following limitations: 1)

The predictions depend heavily on some hydrodynamic parameters; the correlations for these parameters had not been developed at the time the work was done. Only by adjusting these parameters, have fits of the model to the experimental observations been obtained. 2) Experimental observations indicate that the water-gas shift reaction equilibrium is usually not achieved in fluidized-bed gasifiers.

Bacon and Downie (1982) developed a mathematical model for the fluidized-bed gasification of wood. Their model includes wood devolatilization in addition to the char gasification and the water-gas shift reactions considered by Yoshida and Kunii. The model employs the bubble assemblage model and is limited to the bed section. They have assigned varying degrees of equilibrium to the char gasification reactions, thus eliminating kinetic rate expressions from the model. They have assumed that devolatilization occurs instantaneously and that the char gasification reactions occur only in the emulsion phase. Sensitivity analyses have been performed on the model parameters and the operating variables. They have stated that a comparison of the simulated runs with some industrial data exhibits fairly good agreement. A major limitation of the model is that the kinetic rate expressions are not included.

Raman *et al.* (1981) have developed a model to simulate the fluidized-bed gasification of biomass and applied it to

the gasification of feedlot manure. Kinetic rate expressions for the char gasification and water-gas shift reactions as well as hydrodynamic relationships have been extensively employed in modeling the bed. The model also accounts for devolatilization, which is assumed to be instantaneous. No elutriation of char is considered. They have also assumed that devolatilization takes place uniformly throughout the bed. A comparison of the steady gas compositions and experimental results have shown fairly good agreement. The difference between the experimental and simulated results has been attributed to the fact that freeboard reactions and tar cracking reactions are not included. Chang et al. (1983) have extended this work to provide information on dynamic simulations of the fluidized-bed gasifier. The major limitation of the model is that the freeboard reactions are not included in the model.

In the present experimental set-up wood is fed to the top surface of a bed, comprised of an inert solid and char, which is fluidized by steam. Devolatilization takes place instantaneously as the feed contacts the bed surface. The char produced provides char feed to the bed section and the volatiles produced enter the freeboard. Freeboard reactions along with the fact that devolatilization occurs at the surface of the bed have not been considered in earlier modeling studies. These features have been partially accounted for in the present work. The model predictions are

compared with experimental results for the steam gasification of Siberian elm.

MODEL DEVELOPMENT

The model has been developed for isothermal conditions with no elutriation of char. The gasifier is divided into three sections: the bed, the devolatilization and the freeboard sections as illustrated in Figure 4.1. The bed consists of two phases: the bubble and emulsion phases (see Figure 4.2). On the surface of the bed, where feeding of wood occurs, devolatilization takes place. The volatile products completely mix with the product gas exiting the bed and the resultant stream moves up in the freeboard. The char produced in this section provides the char feed for the bed section. The freeboard contains only vapor since elutriation of char is not considered. The particular modeling considerations for each section of the gasifier are detailed in the following sub-sections.

Fluidized-Bed Section

In this section, gasification reactions and interphase mass transport are the important phenomena. The former include the char gasification reactions and the water-gas shift reaction. The interphase mass transfer is affected mainly by the hydrodynamics in the bed. The hydrodynamics of the present model are based on the two phase theory of

fluidization developed by Davidson and Harrison (1963). The conventional assumptions involved in the hydrodynamic aspects of the model include:

1. The fluidized bed consists of two phases, the bubble phase and emulsion phase as shown in Figure 4.2. They are homogeneously distributed, statistically, throughout the bed.

2. The flow of gas in excess of that required for minimum fluidization passes through the bed in the form of bubbles which are free of solids. This implies that char gasification reactions do not take place in the bubble phase.

3. The voidage of the emulsion phase remains constant and is equal to that at incipient fluidization.

4. The bed can be characterized by an equivalent bubble diameter.

5. Plug flow is assumed for the bubble phase gas.

6. The emulsion phase is well mixed.

In addition the following assumptions are imposed on the bed section.

1. The bed is isothermal. This assumption is possible because the feeding is started after the bed (originally consisting of inert solids) is heated to the desired operating temperature and maintained at that temperature after the feeding begins by an external heat source.

2. No elutriation of solids takes place.

The bed section includes reactions of char with H_2, CO_2 and H_2O as well as the water-gas shift reaction.

Devolatilization Section

In the present experimental system, which involves small particles and high heating rates, devolatilization is completed almost instantaneously; subsequently, devolatilization is assumed to take place as the feed material contacts the surface of the expanded bed. The gaseous devolatilization product completely mixes with the product gas exiting the bed and the mixed product enters the freeboard. The char produced enters the bed section.

Freeboard Section

In this section, the flow of the gas is assumed to be in plug flow. The water-gas shift reaction is the only chemical reaction considered. Isothermal conditions are also assumed for this section.

KINETIC CONSIDERATIONS

It is well known that gasification of any carbonaceous material takes place in three steps: (1) Devolatilization or pyrolysis of the solid to produce volatile matter, (2) Cracking of volatiles, and (3) Char gasification reactions

and the water-gas shift reaction (Antal et al., 1979; Raman et al., 1981; Chang et al. 1983). The conceptual reaction scheme can be represented as:

(1) Wood $\xrightarrow{\text{Devolatilization}}$ Heavy Volatiles + Char + Gas (CO, CO_2, H_2, H_2O, HC)

(2) Heavy Volatiles $\xrightarrow{\text{cracking}}$ Lighter Volatiles + Gas

(3) Char Gasification Reactions

$$C + H_2O \xrightarrow{k_1} CO + H_2$$

$$C + CO_2 \xrightarrow{k_2} 2CO$$

$$C + 2\,H_2 \xrightarrow{k_3} CH_4$$

Water-Gas Shift Reaction $CO + H_2O \underset{k_5}{\overset{k_4}{\rightleftharpoons}} CO_2 + H_2$

The initial step in the gasification process, devolatilization or pyrolysis, takes place almost instantaneously at the high heating rates encounterd in a fluidized bed. This has been investigated and discussed in detail by Raman et al., (1981) and Antal, (1978). Antal has estimated the time of initial devolatilization and char formation for particles between 75 and 250 microns in size to be less than 0.5 seconds. Thus, it is reasonable to assume that devolatilization is instantaneous and occurs just when the wood particles contact the surface of the expanded bed.

The devolatilization produces heavy volatiles which crack to form lighter volatiles and gas. The kinetics for this step are not available in the literature at the present time;consequently, cracking cannot be considered in the present model. Kinetics for the char gasification and the water-gas shift reactions are well known and available in literature.

DEVELOPMENT OF GOVERNING EQUATIONS AND METHOD OF SOLUTION

General Considerations

In the present experimental system, involving the steam gasification of wood at atmospheric pressure, it has been observed that only eight chemical species, CO, CO_2, H_2, H_2O, CH_4, C_2H_6 and C_3H_8 along with char exist. This gives rise to the necessity for fifteen differential mass balances (7 for the seven gas species in the bubble phase and 7 for the seven gas species in the emulsion phase and 1 for solid char in the emulsion phase) for the bed section alone. However, since C_2H_6 and C_3H_8 are present only in the devolatilization and freeboard sections and do not take part in any reactions, the number of differential mass balances needed for the bed section reduces to 11. The devolatilization zone involves no differential mass balances. In the freeboard, it is assumed that only the water-gas shift reaction takes place. Since there is only one phase in the freeboard, seven differential mass balances are required; one for each

chemical species. The overall system is therefore described by 18 differential equations.

Material Balances

Fluidized-bed section. The net flow of gas in each phase has been approximated by convective and dispersive terms to give rise to parabolic partial differential equations. The dispersive term was employed in the balances because it was required for the software package used to solve the system of PDEs. The numerical values of these terms (D_{ib} and D_{ie}) have been chosen such that they represent nearly plug flow conditions in the bubble phase and well mixed conditions in the emulsion phase.

a. Bubble phase. A mass balance on chemical species i over a volume of $A_b \Delta x$ (see Figure 4.2) in the bubble phase gives

$$\begin{bmatrix}\text{Rate of}\\ \text{Accumulation}\\ \text{of i}\end{bmatrix} = \begin{cases}\text{Rate in of species i by convection}\\ \text{Rate in of species i by dispersion}\\ \text{Rate out of species i by convection}\\ \text{Rate out of species i by dispersion}\\ \text{Rate out of species i by exchange with emulsion phase}\\ \text{Rate of production of species i by reaction}\end{cases}$$

$$\frac{\partial}{\partial t}\ (A_b \Delta x\ C_{ib}) = -D_{ib}A_b\frac{\partial C_{ib}}{\partial x}\Big|_x + D_{ib}A_b\frac{\partial C_{ib}}{\partial x}\Big|_{x+\Delta x}$$

$$U_b A_b C_{ib}|_x - U_b A_b C_{ib}|_{x+\Delta x}$$

$$- A_b \Delta x F_{be}(C_{ib}-C_{ie}) + A_b \Delta x\ R_{ib} \qquad (4.1)$$

Dividing both sides of Equation (1) by $A_b \Delta x$ and taking the limit as $\Delta x \longrightarrow 0$ yields

$$\frac{\partial C_{ib}}{\partial t} = D_{ib}\frac{\partial^2 C_{ib}}{\partial x^2} - U_b\frac{\partial C_{ib}}{\partial x} - F_{be}(C_{ib}-C_{ie})+R_{ib} \qquad (4.2)$$

b. Emulsion phase. A similar mass balance on component i in the emulsion gas yields

$$\epsilon_{mf}\frac{\partial C_{ie}}{\partial t} = D_{ie}\frac{\partial^2 C_{ie}}{\partial x^2} - U_e\frac{\partial C_{ie}}{\partial x} + \frac{A_b F_{be}}{A_e}(C_{ib}- C_{ie}) + R_{ie} \qquad (4.3)$$

Since it has been assumed that solids are completely mixed in the emulsion phase, a material balance on the solids in the bed section yields an equation of the form

$$B\frac{\partial C_s}{\partial t} = (W_{in} - W_{out}) + R_s \qquad (4.4)$$

or

$$\frac{\partial C_s}{\partial t} = \left(\frac{W_{in} - W_{out}}{B}\right) + \frac{R_s}{B} \qquad (4.5)$$

For the solid material in the emulsion phase, C_s is defined as the weight ratio of char to inert solids in the

bed, and B as the total weight of the inert solids in the bed. Additionally, W_{in} and W_{out} are defined as the rates of char input to and output from the bed, respectively. In the present model, elutriation of char is not considered. Thus, W_{out} is set equal to zero and W_{in} is calculated from the feed rate of wood and the char yield from devolatilization.

c. Initial and boundary conditions. The appropriate initial and boundary conditions for gaseous species i in the bubble and emulsion phases and char in the emulsion phase are as follows

$$t = 0;\ 0 \leq x \leq H \qquad \begin{cases} C_{ib} = C_{io} \\ C_{ie} = C_{io} \\ C_s = 0 \end{cases} \tag{4.6}$$

$$t > 0;\ x = 0 \qquad \begin{cases} C_{io} = C_{ib} - \dfrac{D_{ib}}{U_b}\dfrac{\partial C_{ib}}{\partial x} \\ C_{io} = C_{ie} - \dfrac{D_{ie}}{U_e}\dfrac{\partial C_{ie}}{\partial x} \end{cases} \tag{4.7}$$

$$t > 0;\ x = H \qquad \begin{cases} \dfrac{\partial C_{ib}}{\partial x} = 0 \\ \dfrac{\partial C_{ie}}{\partial x} = 0 \end{cases} \tag{4.8}$$

In the mass balances given by Equations 4.2 and 4.3 and the boundary conditions given by Equations 4.6 through 4.8, i = 1 represents CO, 2, CO_2, 3, H_2, 4, H_2O, and 5, CH_4. Since only steam flows at the start, C_{io} is fixed at zero for all

the species except steam. In the present experiments the feed was started at a constant feed rate at time t=0; this is the basis for the initial condition for C_s.

d. Rate expressions. The rate expressions in equations 2, 3 and 5 are given by

$$R_{1b} = R_{4b} = -R_b \tag{4.9}$$

$$R_{2b} = R_{3b} = R_b \tag{4.10}$$

$$R_{5b} = 0 \tag{4.11}$$

$$R_{1e} = S(k_1 C_{4e} + \frac{k_2 C_{2e}}{2}) - R_{sr} \tag{4.12}$$

$$R_{2e} = -S(k_2 C_{2e}) + R_{sr} \tag{4.13}$$

$$R_{3e} = S(k_1 C_{4e} - k_3 C_{3e}) + R_{sr} \tag{4.14}$$

$$R_{4e} = -Sk_1 C_{4e} - R_{sr} \tag{4.15}$$

$$R_{5e} = \frac{1}{2} (Sk_3 C_{3e}) \tag{4.16}$$

$$R_s = -(k_1 C_{4e} + k_2 C_{2e} + \frac{k_3 C_{3e}}{2}) BA_c C_s M_c \tag{4.17}$$

where

$$R_b = k_4 C_{1b} C_{4b} - k_5 C_{2b} C_{3b} \tag{4.18}$$

$$S = \frac{BA_c C_s}{HA(1-\delta)} \tag{4.19}$$

$$R_{sr} = k_4 C_{1e} C_{4e} - k_5 C_{2e} C_{3e} \tag{4.20}$$

e. Hydrodynamic relationships. Various relationships between the variables and the parameters involved in the bed section have been developed previously by other researchers. Using these relationships, the parameters are evaluated as shown below.

1. The bubble diameter, D_b is estimated using the correlation developed by Mori and Wen(1975)

$$D_b = D_{bm} - (D_{bm} - D_{bo})\exp(-0.3\, x/D)$$

where $$D_{bm} = 0.652\ \{A(U_o - U_{mf})\}^{0.4}$$

and $$D_{bo} = 0.00376(U_o - U_{mf})^2$$

In the above, D_{bo} is the initial bubble diameter, and D_{bm} is the maximum bubble diameter. The equivalent bubble diameter, as defined by Kunii and Levenspiel (1969) is calculated at the middle of the expanded bed, x = H/2.

2. The bubble velocity, U_b, is calculated from the correlation proposed by Davidson and Harrison (1963)

$$U_b = (U_o - U_{mf}) + 0.711(gD_b)^{0.5}$$

3. The volume fraction of the bubble phase, δ, is calculated from

$$\delta = (U_o - U_{mf})/U_b$$

4. The emulsion phase gas velocity, U_e, is calculated from

$$U_e = U_{mf}/(1-\delta)$$

5. The gas exchange coefficient between the bubble and emulsion phases, F_{be}, is calculated from the correlation suggested by Kobayashi et al. (1967).

$$F_{be} = 0.11/D_b$$

6. The height of expanded bed, H, is calculated iteratively, from the material balance on the solid as

$$H = \frac{H_{mf}}{(1-\delta)}$$

Devolatilization section. As explained earlier, devolatilization is nearly instantaneous and takes place at the surface of the bed, generating volatiles and char. Devolatilization data, consisting of the char yield, gas yield and gas compositions, have been taken from an unpublished thesis (Dewyke, 1989) which gives fluidized-bed pyrolysis results for Siberian elm at a temperature of 873 K (see Table 4.3).

The gaseous devolatilization products are added to the gaseous effluent from the bed section; this then specifies the gas composition entering the freeboard. Char produced provides feed to the bed section.

Freeboard section. The gas in the freeboard is assumed to be in plug flow. Since the freeboard contains a single phase(gas), only the water-gas shift reaction need be considered. The governing mass balance is

$$\frac{\partial C_i}{\partial t} = - U_f \frac{\partial C_i}{\partial x_f} + R_{if} \qquad (4.21)$$

where

$$R_{2f} = R_{3f} = k_4 C_{1f} C_{4f} - k_5 C_{3f} C_{5f}$$

$$R_{1f} = R_{4f} = - R_{2f}$$

and i = 1-5 represent the gas species previously defined. Equation 21 is also applicable to the non-reacting

components, C_2H_6 (i=6) and C_3H_8 (i=7) with the generation term set equal to zero. Inlet conditions for the freeboard section are discussed in the next section.

Method of Solution

For the bed section, there are eleven nonlinear partial differential equations that must be solved simultaneously. Their solution yields the transient product gas composition exiting the top of the bed. The simultaneous equations were solved using a PDE solving software package PDEPAC. The "Method of Lines" technique was used for spatial discretization to convert the nonlinear partial differential equations into a system of time dependent nonlinear ODEs. Time integration of the resultant equations yields the gas composition for a given axial position at successive time intervals. The number of moles of each component leaving the bed section (obtained from the integration) is added to the devolatilization product at each time interval.

The above treatment yields the inlet gas composition for the freeboard section. The average of two gas compositions obtained for two successive time intervals is used as the the inlet condition for the freeboard for the entire period between the two time intervals. (For example, the average of the compositions at time t=0 and t=1 serves as the inlet condition for the freeboard region for the time period $0<t<1$). A time integration of equation (4.21) yields the

concentration of component i exiting the freeboard. It should be noted that the dynamic solutions include the steady gas compositions which can be compared with experimental results.

Figure 4.3 presents a schematic representation of the computational procedures for the overall model.

SIMULATION

The experimental system has been described in detail in the previous chapter. Figure 4.4 illustrates the configuration of the reactor. The operating procedure is also detailed in the previous chapter.

The present model employs some simplifications of the actual conditions in the experimental set-up. In the model elutriation of char has not been considered whereas in the actual system char elutriation takes place. It has also been assumed that no char gasification reactions take place in the bubble phase or the freeboard. However, there is a possibility of small amounts of char in the bubble phase undergoing gasification in the bed as well as the gasification of entrained char in the freeboard. In the development of the model, it has also been assumed that there is perfect mixing of the devolatilization gas and the gas exiting the bed surface. Furthermore, tar cracking reactions in the freeboard have not been considered whereas they definitely take place in the actual system.

The range of operating conditions for the experimental runs are summarized in Table 4.1. These conditions are taken as the basis for the simulations. The kinetic parameters and other data for the simulations are summarized in Tables 4.2 and 4.3.

RESULTS AND DISCUSSION

Wood gasification has been simulated by equations 4.1 through 4.21. The residence time in the freeboard is maintained between 4 to 6 seconds to be compatible with experiments. The simulated steady gas compositions are compared with the experimental observations.

The time dependence of simulated gas compositions (exiting the freeboard) at two different temperatures is illustrated in Figures 4.5 and 4.6. The figures indicate that steady gas compositions are reached within 10 seconds. This can be attributed to the fact that the quantity of char is small; consequently,the transient period is dependent primarily on the devolatilization step and the hydrodynamics of the bed. As mentioned earlier, devolatilization is nearly instantaneous; so steady gas compositions are achieved very rapidly. The experimental set-up was not designed for determination of transient gas compositions. Thus, only steady gas compositions can be compared with the simulated results.

Comparisons of typical dry gas compositions (exiting the freeboard) at different temperatures with the experimental results are presented in Tables 4.4a, 4.4b and 4.4c. For each temperature, the same devolatilization data (see Table 4.3) have been employed. The tables indicate that at all temperatures, the model predicts lower CO and slightly higher H_2 than the experimental observations. At higher temperatures, where the water-gas shift reaction dominates, a closer agreement between the experimental and simulated gas compositins and gas yields is observed.

The simulated char content of the bed is shown in Figure 4.7. Note that although steady gas compositions are achieved, the simulated char content of the bed continues to increase with time. This is because elutriation of char from the bed has not been taken into account in the present model. Also, note that increasing the temperature reduces the char content of the bed. The feed rate is constant for both of the simulation runs presented in Figure 4.7. The reduction in the char content with increasing temperature can be attributed to the fact that the char gasification reactions become increasingly pronounced as the temperature is elevated.

The axial concentration profiles for the gas components in the bubble and emulsion phases are illustrated in Figure 4.8. It is evident that the concentrations of H_2, CO, and CO_2 increase with the bed height in the bubble phase and

approach steady values approximately equal to those of the emulsion phase concentration. This implies intensive interphase mixing under the simulated operating conditions.

As explained earlier, the model takes into account devolatilization at the bed surface and partially accounts for freeboard reactions of the gaseous products. These conditions have not been considered in earlier models (Raman, 1981; Chang, 1984). To assess the improvement in the model predictions, a simulation has been conducted under Raman's experimental conditions (temperature = 983 K). A comparison between Raman's model predictions and the present model predictions is presented in Table 4.5; it can be seen that the present model gives moderate improvements in the predictions of the concentrations of CO and CO_2 compared to Raman's model.

The present model needs some additional refinements. First, more accurate devolatilization data for Siberian elm need to be obtained. Secondly, cracking of the heavy volatiles needs to be accounted for in the governing equations for the freeboard. Moreover, the model must account for elutriation of char from the bed and its subsequent gasification in the freeboard.

CONCLUDING REMARKS

A mathematical model has been developed for the steam gasification of wood in a fluidized-bed reactor. The model

predicts the transient reactor performance; it indicates that a very short time is required for steady gas compositions to be obtained. The model takes into account devolatilization, char gasification, the shift reaction and partially accounts for freeboard reactions of the gaseous products. The model predictions are compared with the experimental data obtained for the bench-scale, fluidized-bed reactor gasifying Siberian elm. The model predictions represent the observed experimental trends reasonably well.

NOMENCLATURE

A_b = cross sectional area of reactor in bubble phase, m^2

A_e = cross sectional area of reactor in emulsion phase, m^2

A_c = surface area of char, m^2/kg

B = weight of inert solids in the bed, kg

C_{ib} = concentration of species i in bubble phase, $kmol/m^3$

C_{ie} = concentration of species i in emulsion phase, $kmol/m^3$

C_{if} = concentration of species i in freeboard, $kmol/m^3$

C_{io} = inlet concentration of species i, $kmol/m^3$

C_s = concentration of char in emulsion phase, kg char / kg inert solids

D = diameter of the reactor, m

D_{ib} = axial dispersion coefficient in bubble phase, m^2/s

D_{ie} = axial dispersion coefficient in emulsion phase, m^2/s

D_b = bubble diameter, m

D_{bm} = maximum bubble diameter, m

D_{bo} = initial bubble diameter, m

F = dry ash free feed rate, kg/s

F_{be} = gas interchange coefficient between emulsion and bubble phases based on volume of bubbles, 1/s

H = bed height, m

H_{mf} = bed height at minimum fluidization, m

M_c = atomic weight of carbon, 12 kg/kmol

R = gas constant, 1.987 kcal/kmol. K

R_{ib} = rate of generation of species i based on volume of bubbles, $kmol/m^3.s$

R_{ie} = rate of generation of species i based on volume of emulsion phase, $kmol/m^3.s$

R_{if} = rate of generation of species i based on volume of freeboard, $kmol/m^3.s$

R_s = rate of generation of char in emulsion phase, kg/s

t = time, s

T = temperature, K

U_b = bubble rise velocity, m/s

U_e = superficial velocity of emulsion gas based on cross sectional area of emulsion phase, m/s

U_{mf} = superficial gas velocity at minimum fluidization, m/s

U_f = velocity of gas in freeboard, m/s

W_{in} = rate of char generation by devolatilization, kg/s

W_{out} = rate of char out of the reactor, kg/s

x = axial distance from the distributor, m

x_f = axial distance from the top of the expanded bed, m

Subscripts

i = indices specifying species (1= CO; 2 = CO_2; 3 = H_2; 4 = H_2O; 5 = CH_4; 6 = char)

j = indices indicating the reactions

Greek Letters

δ = volume fraction of the bubble phase

ρ = density of solids in the reactor, kg/m^3

ϵ_{mf} = void fraction of the bed at minimum fluidization

REFERENCES

Antal, M. J., W. E. Edwards, H. L. Friedman, and F. E. Rogers, "A Study of the Steam Gasification of Organic Wastes," Project Report to EPA, W. W. Liberick, Project Officer, 1978.

Antal, M. J., "The Effects of Residence Time, Temperature, and Pressure on the Steam Gasification of Biomass", presented at the Symposium on Biomass as a Non-Fossil Fuel Source, Div. of Fuel Chem. ACS meeting, Honolulu, April 1-6, 1979.

Bacon, D. W., J. Downie, J. C. Hsu, and J. Peters, "Modeling of Fluidized Bed Wood Gasifiers," presented at the Fundamentals of Thermochemical Biomass Conversion Conference, Estes Park, CO, Oct. 18-22, 1982.

Chang, C. C., L. T. Fan, and W. P. Walawender, "Dynamic Modeling of Biomass Gasification in a Fluidized Bed," presented at AIChE Annual meeting, Washington D.C., Oct.30-Nov.4, 1983. Also in AIChE Symp. Series, 80, 80-90 (1984).

Davidson, J. F., and D. Harrison, "Fluidized Particles," Cambridge University Press, New York, 1963.

Dewyke, J., thesis in preparation, Kansas State University, 1989.

Kobayashi, H., and F. Arai, "Determination of Gas Cross Flow Coefficient between the Bubble and Emulsion Phases by Measuring the Residence Time Distribution of Fluid in a Fluidized Bed," Kagaku Kogaku, 31, 239 (1967).

Kunii, D., and O. Levenspiel, "Fluidization Engineering," Chapter 4, Wiley, New York, 1969.

Mori, S., and C. Y. Wen, "Estimation of Bubble Diameter in Gaseous Fluidized Beds," AIChE Journal, 21, 109-115 (1975).

Raman, K. P., W. P. Walawender, L. T. Fan, and C. C. Chang, "Mathematical Model for the Fluid Bed Gasification of Biomass Materials. Application to Feedlot Manure," Ind. Eng. Chem. Process Des. Dev., 20, 686-692 (1981).

Yasihida, K., and D. Kunii, "Complex Reactions in Fluidized Bed - Simulation and Gasification," Chem. Eng. Sci, 7, 34-39 (1974).

Yoon, H., J. Wei., and M. M. Denn, "Modeling and Analysis of Moving Bed Coal Gasifeirs," AF-590, Vol. 1, Technical Planning Study 76-653, Research Project 986-1, Final Report, 1977.

Table 4.1. Reactor Operating Parameters.

Reactor Temperature Range (K)		850 - 1125
Fluidizing Gas		Steam
Superficial Velocity	(m/s)	0.14 - 0.165
Condensate Rate	(cc/min)	9.0 - 17
Feed Rate	(DAF gm/min)	0.9 - 4.0
U_{mf}	(m/s)	0.09-0.12
ε_{mf}		0.43
D_{ib}	(m^2/s)	0.001
D_{ie}	(m^2/s)	1000
Bed Height	(m)	0.08

Table 4.2. Kinetic Parameters for the Reactions.

Reactions	Activation Energy (E_j) KJ/Kmol	Adjusted Freq. Factor(k_j^o)m/hr
$C - H_2O \xrightarrow{k1} CO + H_2$	121,417	$5.0 * 10^2$
$C + CO_2 \xrightarrow{k2} 2CO$	360,065	$0.2 * 10^9$
$C + 2H_2 \xrightarrow{k3} CH_4$	230,274	$0.75 * 10^3$
$CO + H_2O \xrightarrow{k4} CO_2 + H_2$	12,560	$0.1 * 10^8$
$CO + H_2O \underset{k5}{\overset{k4}{\rightleftharpoons}} CO_2 + H_2$	$k_w = k4/k5 = 0.0265$	$(m^3/kmolhr)$ exp(3955/T)[a]

[a] Yoon (1977)

Table 4.3. Devolatilization Product distribution for wood at temperature = 873 K*

Product	%
Char (wt % DAF)	15
Dry Gas (wt % DAF)	63
Dry Gas Composition (vol %)	
CO	22
H_2	36
CO_2	29
CH_4	9
Others	4

* Dewyke (1989)

Table 4.4 a. Comparison of Experimental and Simulated Steady Gas Compositions(temperature=943K).

Response Variable	Simulated	Experimental
mole % CO	7.2	18.1
mole % CO_2	37.1	28.3
mole % H_2	52.4	42.1
dry gas mass yield	0.77	0.72

Table 4.4 b. Comparison of Experimental and Simulated Steady Gas Compositions(temperature=993K).

Response Variable	Simulated	Experimental
mole % CO	6.4	12.2
mole % CO_2	33.7	29.4
mole % H_2	58.2	47.4
dry gas mass yield	0.79	0.87

Table 4.4 c. Comparison of Experimental and Simulated Steady Gas Composition(temperature=1043K).

Response Variable	Simulated	Experimental
mole % CO	4.1	8.4
mole % CO_2	33.7	30.3
mole % H_2	61.1	53.3
dry gas mass yield	0.89	1.01

Table 4.5. Comparison of Present Model Predictions with previous models(temperature=983K).

Response Variable	Present Model	Raman's Model*	Expt. Value*
Mole % CO	10.68	8.0	18.15
Mole % CO_2	57.32	62.9	34.82
Mole % H_2	23.82	23.6	35.0

* Obtained from "Mathematical model for fluid-bed gasification of biomass materials. Application to Feedlot Manure", I&EC Process Design & Development, 20, 690 (1981).

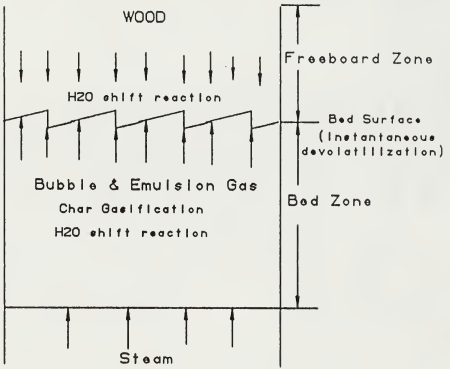

Figure 4.1. Schematic representation of the model indicating the three zones.

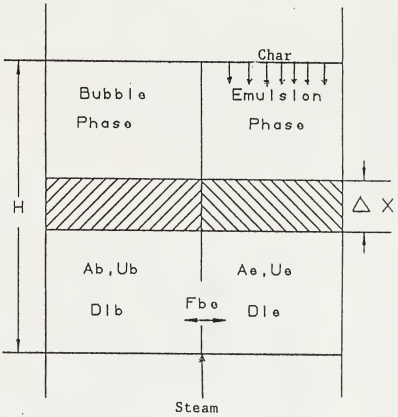

Figure 4.2. Schematic representation of the bed section indicating bubble and emulsion phases.

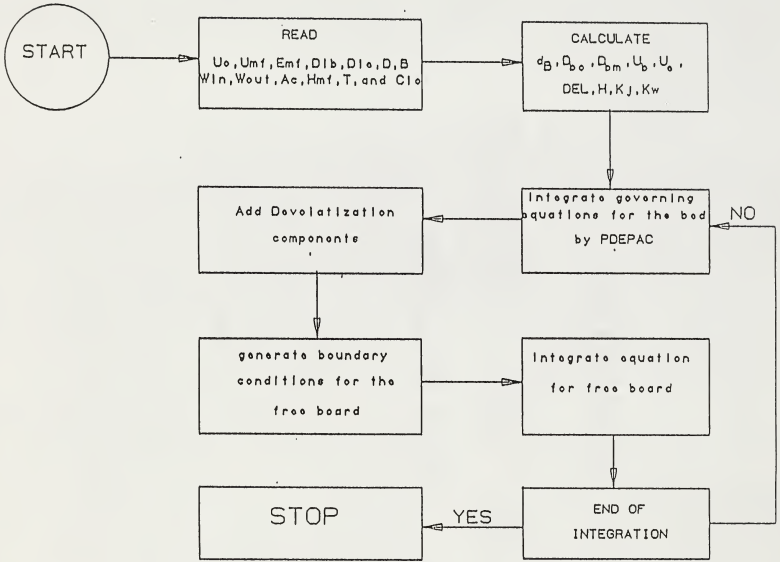

Figure 4.3. Flow diagram of computation.

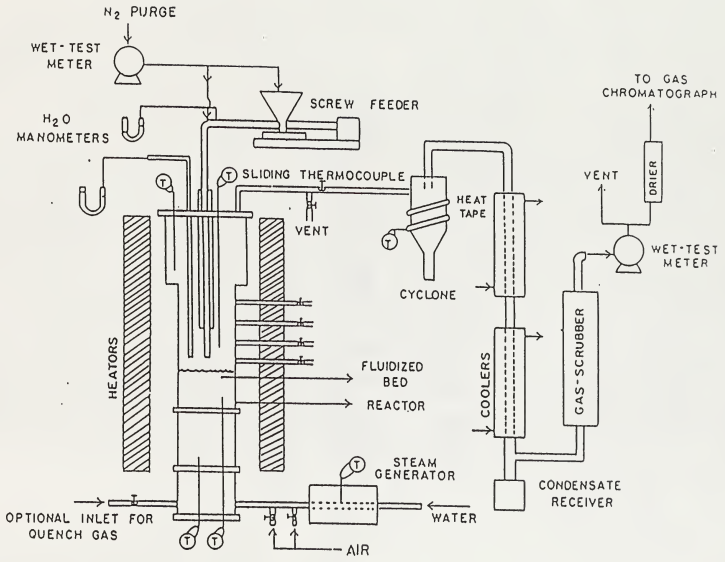

Figure 4.4. Bench scale fluidized bed wood gasification system.

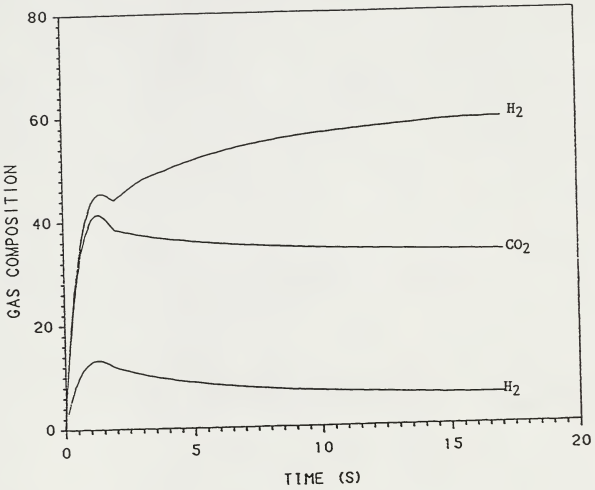

Figure 4.5. Simulated gas composition as a function of time. at temperature = 993K.

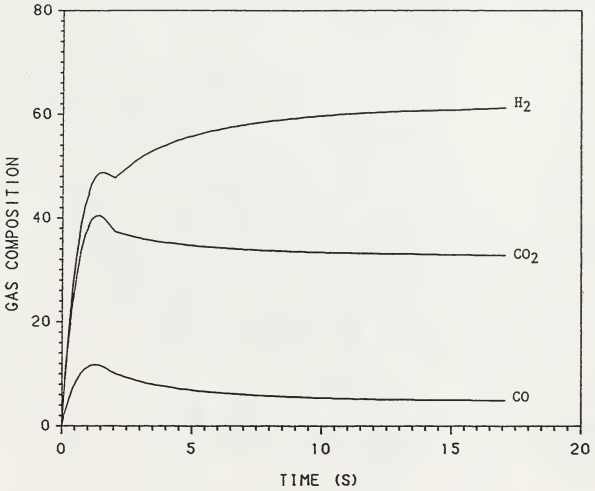

Figure 4.6. Simulated gas composition as a function of time at temperature = 1043 K.

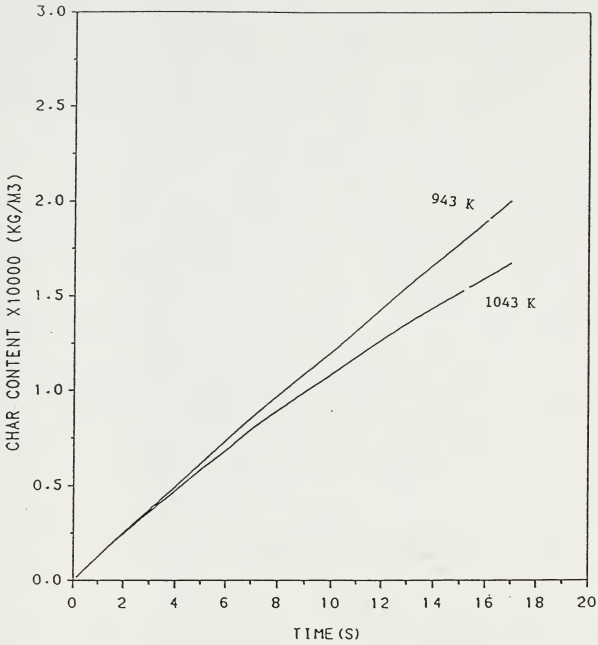

Figure 4.7. Char content in the bed as a function of time at two different temperatures.

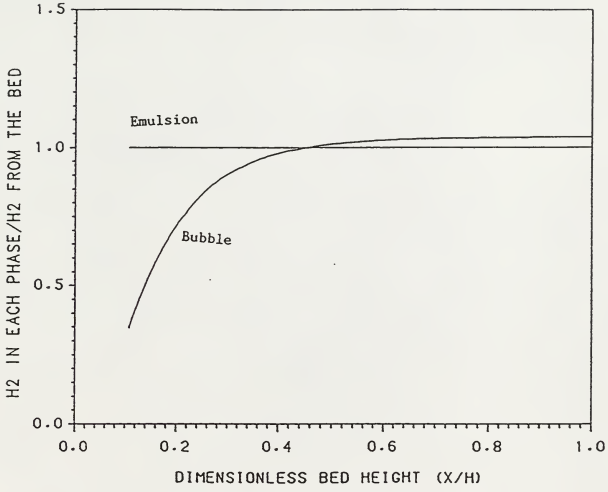

Figure 4.8.. Axial Distribution of H_2 Concentration in each Phase with a Reactor Temperature of 943 K.

CHAPTER 5

CONCLUSIONS AND RECOMMENDATIONS

Gasification experiments were conducted in an experimental fluidized-bed reactor with ground Siberian elm as the feed material. Steam was employed as the sole fluidizing agent at different steam-to-feed ratios. The operating temperature was varied between 850 K and 1150 K. The gasification characteristics of interest were the gas composition, the higher heating value of the gas, the volumetric and mass yields of the product gas, the carbon conversion and the energy recovery. The gas phase residence time was held nearly constant in all the experiments.

For temperatures above 940 K, the experimental results indicated that the process was dominated by the water-gas shift reaction. Steam, which was present in large excess, was found to be a significant gasification agent taking part. Additionally, multiple regression analysis revealed that the steam-to-feed (S/F) ratio was an important factor in determining the product gas compositions and yield. An increase in the S/F ratio resulted in an increase in the concentration of H_2, a decrease in the concentration of CO, and increases in the volumetric and mass yields of gas. These trends were consistent with the water-gas shift reaction postulation.

A mathematical model has been developed to describe the dynamic characteristics of the gasifier. The model accounts for wood devolatilization, the char gasification reactions, the water-gas shift reaction, and the freeboard reactions.

The model predicts both transient and steady gas compositions. The steady gas compositions compare reasonably well with the experimental observations.

Some modifications are recommended for the present experimental system. The major drawbacks of the experimental set-up are the fluctuations in the temperature profile and the feed rate. A uniform feed rate might help to reduce data scatter. Higher density feed materials or an improved feeding system can aid in reducing feed-rate fluctuations. Computer control of the temperature in the reactor can help to reduce the variations in the temperature profile.

In further studies, the steam gasification of the major wood constituents should be systematically studied. Wood consists of three major constituents: cellulose, lignin and hemicellulose. Their relationship to the observed gasification behavior needs to be established. Preliminary work on the steam gasification of cellulose has been conducted; lignin has not yet been successfully gasified. The present experimental set-up could be employed for studying lignin gasification; however, a larger feed pipe needs to be used to prevent clogging of the feed pipe. Also, experiments with other wood species are recommended for establishing relationships between the gasification behavior and wood composition.

The present experimental set-up can also be used to establish the effect of residence time on the product gas

characterisitics. Changing the superficial velocity and thereby altering the volatiles residence time can be used to establish kinetics for the thermal cracking of tar.

The present model does not account for tar cracking in the freeboard. Incorporating cracking into the model and obtaining precise devolatilization data will improve the model. Very short residence time experiments can minimize tar cracking and provide devolatilization product characteristics. Elutration of char also needs to be considered in the model.

STEAM GASIFICATION OF SIBERIAN ELM

by

GANESAN SUNDAR

B.Tech. Indian Institute of Technology, Madras, 1985

AN ABSTRACT OF A MASTER'S THESIS

submitted in partial fulfillment of the
requirements for the degree

MASTER OF SCIENCE

Department of Chemical Engineering

KANSAS STATE UNIVERSITY
Manhattan, Kansas

1988

Gasification experiments were conducted in a bench-scale fluidized-bed reactor; ground Siberian elm served as the feed material. Steam was employed as the sole fluidizing agent at different steam-to-feed mass ratios. The operating temperature was varied between 900 K and 1150 K while the gas phase residence time was held nearly constant. The gasification characteristics of interest were the gas composition, the higher heating value of the product gas, the volumetric and mass yields of the product gas, the carbon conversion and the energy recovery.

For temperatures above 940 K, it has been proposed that the water-gas shift reaction dominates the gasification process. The results of the present work lend further support to this hypothesis. Additionally, multiple regression analyses were used to asses the effect of steam-to-feed (S/F) ratio on the gasification characteristics. The S/F ratio was found to be an important factor in determining the product characteristics. An increase in this ratio resulted in increases in the yield of H_2, a reduction in the yield of CO, increases in the mass and volumetric yields of gas, and an increase in the energy recovery. All these trends are consistent with the water-gas shift reaction postulation.

Steam gasification provides a means for converting wood into a hydrogen-rich gas that can be used as a utility fuel or for chemical synthesis. By varying the steam-to-feed

ratio, the gas composition can be adjusted for specific chemical synthesis such as methanol synthesis. This can be accomplished without catalysts.

A mathematical model has been developed to describe the dynamic behavior of the reactor. The model accounts for wood devolatilization, the char gasification reactions, the water-gas shift reaction, and the freeboard reactions. The model simulates both the transient and steady-state gas compositions. The steady-state gas composition compare reasonably well with the experimental observations.